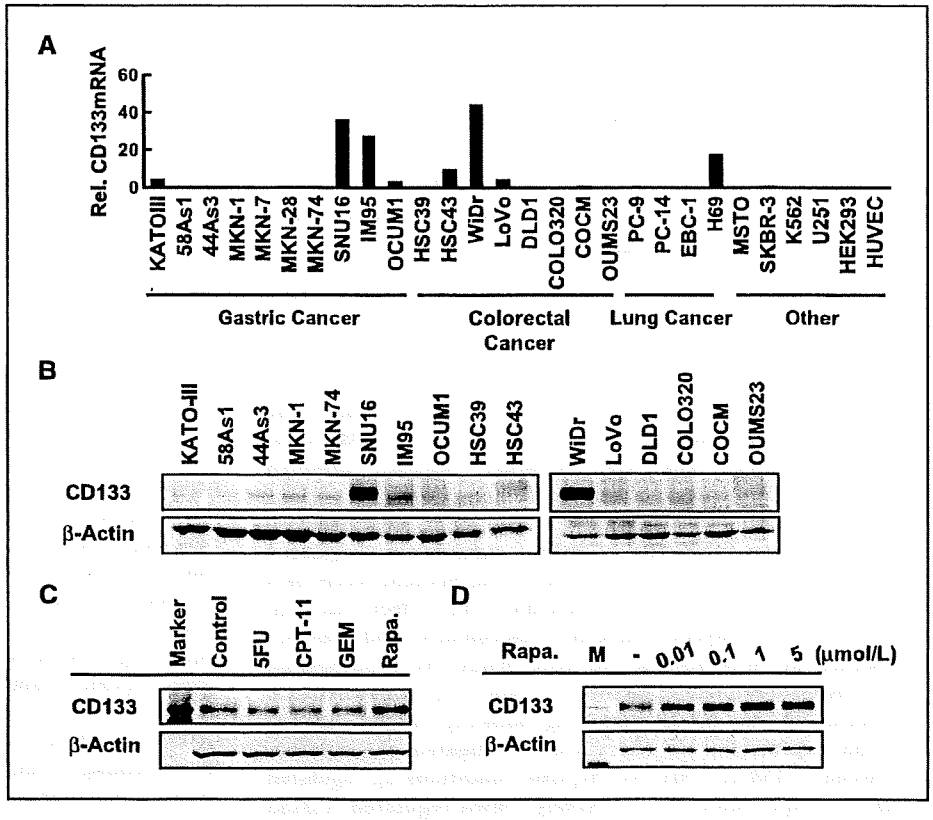

Figure 1. Rapamycin up-regulates CD133 expression. *A*, the mRNA expression levels of CD133 were examined using real-time RT-PCR in 26 cancer cell lines. *B*, the protein expressions of CD133 were determined using Western blotting in 16 gastric and colorectal cancer cell lines. *C*, Western blot of CD133 expression in WiDr cells exposed to cytotoxic drugs [1 μmol/L of 5-fluorouracil (*5-FU*), CPT-11, and gemcitabine (*GEM*)] and rapamycin (1 μmol/L) for 48 h. Note that only rapamycin up-regulates CD133 expression. *D*, WiDr cells were exposed to rapamycin at the indicated concentrations (0, 0.01, 0.1, 1, and 5 μmol/L) for 48 h. Rapamycin dose-dependently up-regulated CD133 expression. *Rel. CD133 mRNA*, normalized mRNA expression levels (CD133/GAPD × 10^4); *Rapa.*, rapamycin.

Immunoblotting. A Western blot analysis was performed as described previously (10). The experiment was performed in triplicate. The following antibodies were used: monoclonal CD133 antibody (W6B3C1; Miltenyi Biotec), rabbit polyclonal HIF-1α antibody (Novus Biologicals, Inc.), β-actin antibody, and HRP-conjugated secondary antibody (Cell Signaling Technology).

Results

Inhibition of the mTOR signal up-regulates CD133 expression in CD133-overexpressing gastrointestinal cancer cells. We examined the mRNA expression levels of CD133 in 26 cancer cell

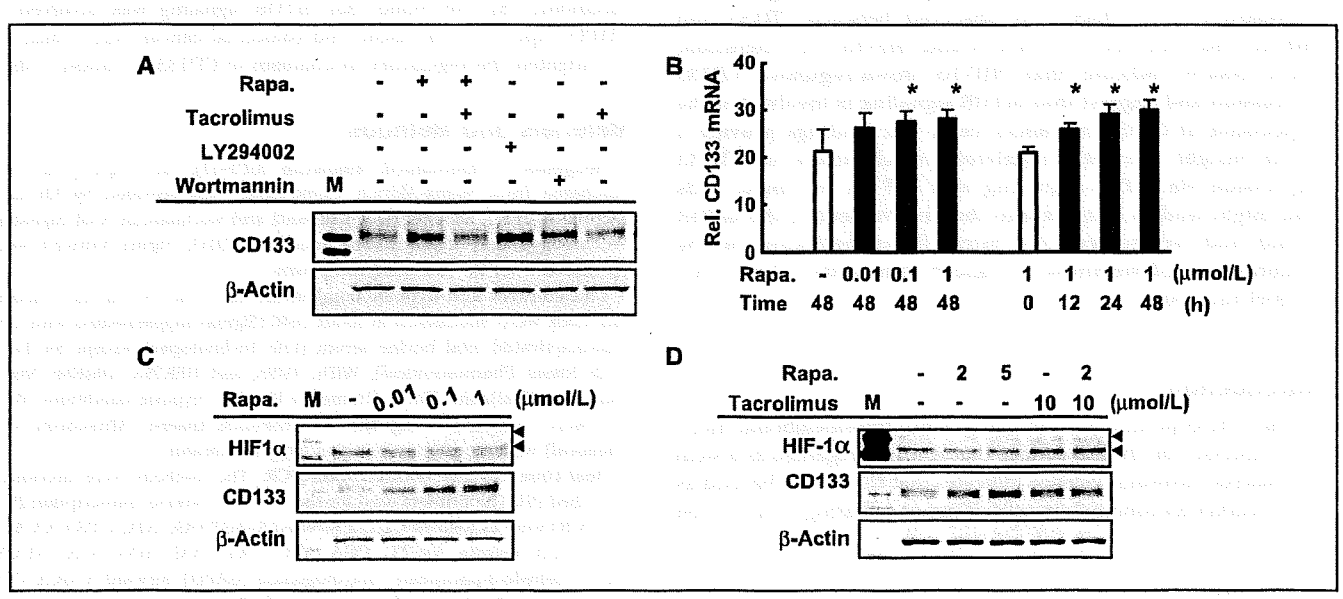

Figure 2. Rapamycin down-regulates HIF-1α expression and up-regulates CD133 expression at the transcriptional level. *A*, WiDr cells were exposed to rapamycin, the rapamycin-competitor tacrolimus, and the phosphoinositide-3-kinase inhibitors LY294002 and wortmannin for 48 h at concentrations of 10 μmol/L. The inhibition of mTOR signaling up-regulated CD133 expression. *B*, rapamycin up-regulated the expression of CD133 mRNA in WiDr cells in a time-dependent and dose-dependent manner. *Columns*, mean determined using real-time RT-PCR; *bars*, SD. *C* and *D*, rapamycin exposure and HIF-1α expression. WiDr cells were exposed to rapamycin with/without tacrolimus at the indicated concentration for 48 h. Rapamycin down-regulated HIF-1α expression and inversely up-regulated CD133 expression; these effects were canceled by tacrolimus. *Rel. CD133 mRNA*, normalized mRNA expression levels (CD133/GAPD × 10^4); *Rapa.*, rapamycin.

lines using real-time RT-PCR. Several gastric, colorectal, and lung cancer cell lines such as SNU16, IM95, HSC43, WiDr, and H69, overexpressed CD133 (Fig. 1*A*). The increased expression of CD133 protein was also confirmed in these cell lines (Fig. 1*B*). The mTOR inhibitor rapamycin, but not cytotoxic drugs (5-fluorouracil, CPT-11, and gemcitabine), increased the expression of CD133 in a dose-dependent manner in CD133-overexpressing WiDr cells (Fig. 1*C* and *D*). These results indicate that mTOR signaling is involved in the expression of CD133 in cancer cells.

Rapamycin down-regulated HIF-1α expression and up-regulated CD133 expression at the transcriptional level. To examine the signal transduction of rapamycin-induced CD133 expression, we used the rapamycin-competitor tacrolimus and the phosphoinositide-3-kinase inhibitors LY294002 and wortmannin. Tacrolimus (10 μmol/L) completely canceled the up-regulation of CD133 induced by rapamycin. The inhibition of phosphoinositide-3-kinase by LY294002 (10 μmol/L) and wortmannin (10 μmol/L) also up-regulated CD133 expression (Fig. 2*A*). Rapamycin up-regulated CD133 expression at the transcriptional level in a dose-dependent and time-dependent manner (Fig. 2*B*).

The inhibition of mTOR signaling is likely to lead to the down-regulation of the expression of certain molecules because the mTOR complex positively regulates the general translational machinery. Under the inhibition of mTOR signaling, HIF-1α, among several downstream molecules of mTOR, can activate transcription by acting as a repressor of specific transcription factors such as the MYC-associated protein X homodimer (11). Therefore, we focused on the possible role of HIF-1α in the regulation of CD133 expression. Rapamycin down-regulated HIF-1α expression but up-regulated CD133 expression (Fig. 2*C*). Meanwhile, tacrolimus canceled the effect of rapamycin on the expressions of HIF-1α and CD133 (Fig. 2*D*). These results suggest that the down-regulation of HIF-1α may mediate the up-regulation of CD133 expression in cancer cells. Up-regulation of CD133 expression by rapamycin was reproducibly observed in the CD133 high-expressing cell lines, but not in CD133 low-expressing cell lines (Supplemental Fig. S2).

Induction of HIF-1α down-regulates CD133 expression in cancer cells. Hypoxia mediates the stabilization of HIF-1α protein and enables its escape from rapid degradation, facilitating the up-regulation of HIF-1α expression (12). Hypoxia strongly induced HIF-1α expression, whereas CD133 expression was down-regulated in all three CD133-overexpressing cell lines (Fig. 3*A*). Rapamycin dose-dependently up-regulated CD133 expression under normoxic conditions, but no effect was seen under hypoxic conditions. We speculated that the effect of hypoxia on the induction of HIF-1α is much higher than the effect of rapamycin on the down-regulation of HIF-1α. The expression of CD133 mRNA was also strongly down-regulated under hypoxic conditions in all three cell lines (Fig. 3*B*) and in three additional cell lines (Supplemental Fig. S1).

In addition, DFO, a known HIF-1α activator, induced HIF-1α expression in a dose-dependent manner but down-regulated the expression of CD133 at both the mRNA and protein levels in WiDr cells (Fig. 3*C* and *D*), and in three additional cell lines (Supplemental Fig. S2). These results were consistent with those obtained under hypoxic conditions. Both hypoxia and DFO exposure markedly down-regulated CD133 expression, strongly suggesting that induction of HIF-1α results in the down-regulation of CD133 expression.

Inverse correlation between CD133 and HIF-1α in clinical samples. Finally, to address whether CD133 and HIF-1α expression are inversely correlated in clinical samples of gastric cancer

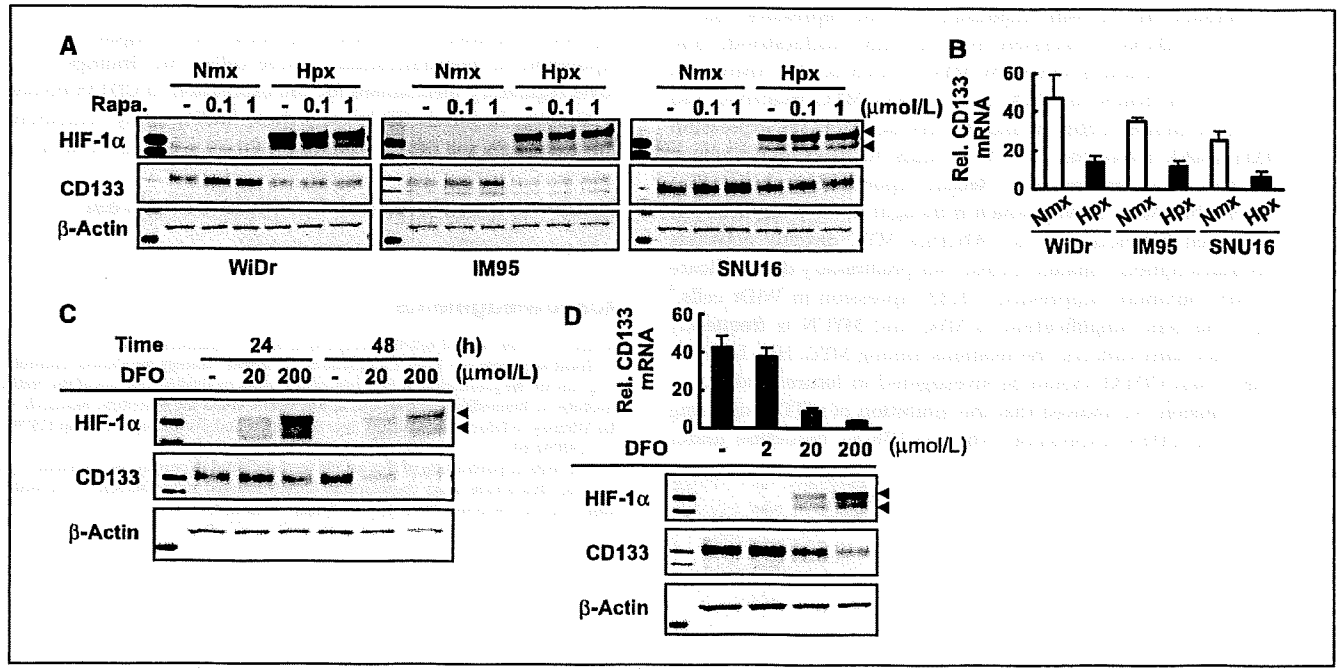

Figure 3. Induction of HIF-1α down-regulates CD133 expression in cancer cells. *A*, three gastrointestinal cancer cell lines were exposed to rapamycin under normoxic or hypoxic conditions for 24 h. Hypoxia induced HIF-1α expression and inversely down-regulated CD133 expression. *B*, hypoxia strongly down-regulated CD133 expression at the mRNA level. *Columns*, mean determined using real-time RT-PCR; *bars*, SD. *C*, DFO, a known HIF-1α activator, induced HIF-1α expression and down-regulated CD133 expression in WiDr cells. *D*, DFO induced these effects at both the mRNA and protein levels. Note that both hypoxia and DFO exposure had similar effects on HIF-1α induction and CD133 down-regulation. *Rel. CD133 mRNA*, normalized mRNA expression levels (CD133/GAPD × 10^4); *Rapa.*, rapamycin.

specimens, we examined the expression of these molecules using previously published microarray data (9). The expressions of CD133 and HIF-1α were inversely correlated in gastric cancer ($r = -0.68$; Fig. 4*A*), whereas the expressions of CD133 and HIF-1β were not ($r = -0.05$; Fig. 4*A*). These results are consistent with the *in vitro* findings in the present study.

Taken together, the present results suggest that an oxygen-sensitive intracellular pathway involving both HIF-1α and mTOR signaling may, at least in part, regulate CD133 expression in cancer cells (shown in the schema in Fig. 4*B*).

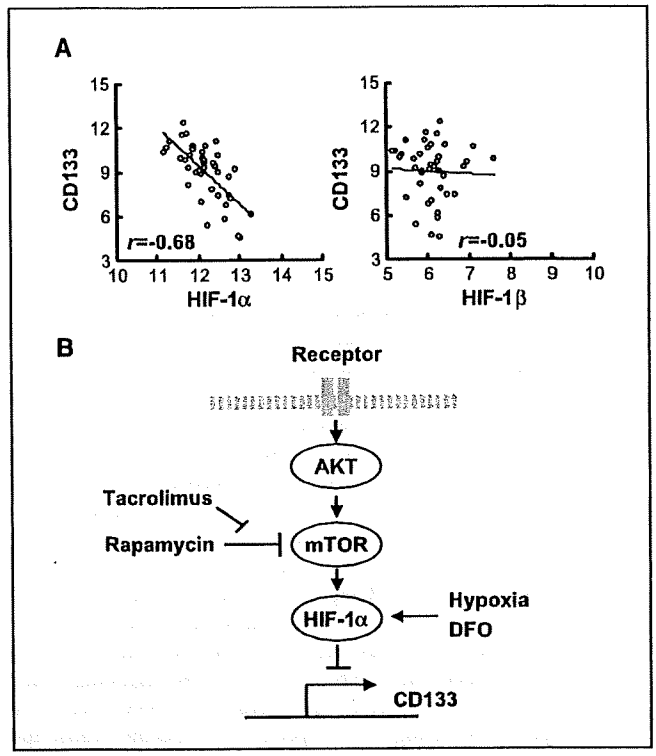

Figure 4. Inverse correlation between CD133 and HIF-1α in clinical samples of gastric cancer. *A*, the correlation between the expressions of CD133 and HIF-1α were analyzed in 40 clinical gastric cancer specimens using previously published microarray data. CD133 and HIF-1α were inversely correlated in gastric cancer ($r = -0.68$), whereas CD133 and HIF-1β were not ($r = -0.05$). *B*, proposed model depicting the involvement of mTOR signaling, HIF-1α, and CD133 expression. HIF-1α, a downstream molecule of mTOR, down-regulates CD133 expression at the transcriptional level in cancer cells.

Discussion

Hypoxic conditions promote the proliferation of mammalian ES cells more efficiently than normoxia and are thought to be required for the maintenance of full pluripotency. Hematopoietic stem cells are located in the bone marrow, which is a physiologically hypoxic environment, and the survival and/or self-renewal of hematopoietic stem cells is enhanced *in vitro* if the cells are cultured under hypoxic conditions (13). Thus, accumulating data indicates that oxygen levels influence specific cell fates in several developmental processes; however, the effect of oxygen levels on cell differentiation is thought to be context-dependent (14). Our data on CD133 expression in response to hypoxia were different from the previous study shown in glioma (5). The discrepancy might be explained by (*a*) a different cellular context in glioma from the others, because CD133 expressions of all cell lines including the WiDr, IM95, SNU16, OCUM1, 44As3, and DLD-1 cells were reproducibly down-regulated by hypoxic condition (Supplemental Fig. S1; Fig. 3*B*), whereas the U251 cells failed to exhibit the down-regulation, and by (*b*) the different detection methods in our study (Western blot and quantitative real-time RT-PCR) from the previous report (flow cytometry for CD133-positive cells).

The detailed mechanism responsible for the repressive role of HIF-1α on CD133 expression is not fully understood; one possible explanation is raised by MYC, which is also known as c-Myc. HIF-1α binds to MAX and renders MYC inactive, and HIF-1 (homodimers of HIF-1α and HIF-1β) activates the expression of MXI1 (MAX interactor 1), which binds to MAX and thereby antagonizes MYC function (11). Recent reports have shown that HIF-1α inhibits MYC activity, which is thought to have implications for stem cell function (15, 16). Whether MYC directly activates CD133 transcription remains unclear; our preliminary data indicate that a MYC-inhibitor suppressed CD133 expression in WiDr cells.[4] Because the gene amplification of MYC and MYCN is frequently observed in many cancers, the relations among MYC, HIF-1α, HIF-1β, HIF-2, and CD133 should be investigated in future studies.

In conclusion, we showed that the inhibition of mTOR signaling up-regulated CD133 expression, whereas HIF-1α induction under hypoxic conditions or DFO exposure down-regulated CD133 expression in gastrointestinal cancer cells. Our findings show a novel regulatory mechanism for the expression of CD133 involving mTOR signaling and HIF-1α, and these findings may contribute to our understanding of the stemness character of cancer stem cells.

[4] Unpublished data.

Disclosure of Potential Conflicts of Interest

No potential conflicts of interest were disclosed.

Acknowledgments

Received 4/7/09; revised 6/2/09; accepted 6/30/09; published OnlineFirst 9/8/09.

Grant support: 3rd Term Comprehensive 10-Year Strategy for Cancer Control, the program for the promotion of Fundamental Studies in Health Sciences of the National Institute of Biomedical Innovation, and a Grant-in-aid for Scientific Research from the Ministry of Education, Culture, Sports, Science and Technology of Japan (19790240 and 19209018).

The costs of publication of this article were defrayed in part by the payment of page charges. This article must therefore be hereby marked *advertisement* in accordance with 18 U.S.C. Section 1734 solely to indicate this fact.

References

1. Neuzil J, Stantic M, Zobalova R, et al. Tumour-initiating cells vs. cancer "stem" cells and CD133: what's in the name? Biochem Biophys Res Commun 2007;355:855–9.
2. Fan X, Matsui W, Khaki L, et al. Notch pathway inhibition depletes stem-like cells and blocks engraftment in embryonal brain tumors. Cancer Res 2006;66:7445–52.
3. Clement V, Sanchez P, de Tribolet N, Radovanovic I, Ruiz i Altaba A. HEDGEHOG-GLI1 signaling regulates human glioma growth, cancer stem cell self-renewal, and tumorigenicity. Curr Biol 2007;17:165–72.
4. Piccirillo SG, Reynolds BA, Zanetti N, et al. Bone morphogenetic proteins inhibit the tumorigenic potential of human brain tumour-initiating cells. Nature 2006;444:761–5.

5. Platet N, Liu SY, Atifi ME, et al. Influence of oxygen tension on CD133 phenotype in human glioma cell cultures. Cancer Lett 2007;258:286–90.
6. Chen HL, Pistollato F, Hoeppner DJ, Ni HT, McKay RD, Panchision DM. Oxygen tension regulates survival and fate of mouse central nervous system precursors at multiple levels. Stem Cells 2007;25:2291–301.
7. Hudson CC, Liu M, Chiang GG, et al. Regulation of hypoxia-inducible factor 1α expression and function by the mammalian target of rapamycin. Mol Cell Biol 2002; 22:7004–14.
8. Chiang GG, Abraham RT. Targeting the mTOR signaling network in cancer. Trends Mol Med 2007;13: 433–42.
9. Yamada Y, Arao T, Gotoda T, et al. Identification of prognostic biomarkers in gastric cancer using endoscopic biopsy samples. Cancer Sci 2008;99: 2193–9.
10. Takeda M, Arao T, Yokote H, et al. AZD2171 shows potent antitumor activity against gastric cancer over-expressing FGFR2/KGFR. Clin Cancer Res 2007;13: 3051–7.
11. Dang CV, Kim JW, Gao P, Yustein J. The interplay between MYC and HIF in cancer. Nat Rev Cancer 2008;8: 51–6.
12. Wouters BG, Koritzinsky M. Hypoxia signalling through mTOR and the unfolded protein response in cancer. Nat Rev Cancer 2008;8:851–64.
13. Danet GH, Pan Y, Luongo JL, Bonnet DA, Simon MC. Expansion of human SCID-repopulating cells under hypoxic conditions. J Clin Invest 2003;112:126–35.
14. Simon MC, Keith B. The role of oxygen availability in embryonic development and stem cell function. Nat Rev Mol Cell Biol 2008;9:285–96.
15. Koshiji M, Kageyama Y, Pete EA, Horikawa I, Barrett JC, Huang LE. HIF-1α induces cell cycle arrest by functionally counteracting Myc. EMBO J 2004;23: 1949–56.
16. Zhang H, Gao P, Fukuda R, et al. HIF-1 inhibits mitochondrial biogenesis and cellular respiration in VHL-deficient renal cell carcinoma by repression of C-MYC activity. Cancer Cell 2007;11:407–20.

ANTICANCER RESEARCH *29*: 1111-1118 (2009)

EGFR Mutation Up-regulates EGR1 Expression through the ERK Pathway

MARI MAEGAWA[1,2], TOKUZO ARAO[1], HIDEYUKI YOKOTE[1], KAZUKO MATSUMOTO[1], KANAE KUDO[1], KAORU TANAKA[1], HIROYASU KANEDA[1], YOSHIHIKO FUJITA[1], FUMIAKI ITO[2] and KAZUTO NISHIO[1]

[1]*Department of Genome Biology, Kinki University School of Medicine, Osaka;*
[2]*Department of Biochemistry, Setsunan University, Osaka, Japan*

Abstract. *Background: DelE746_A750-type EGFR is a constitutively active type of mutation that enhances EGFR signaling. However, the changes in gene expression that occur in mutant EGFR-harboring cells has not been fully studied. Materials and Methods: A gene expression analysis of HEK293 cells transfected with wild-type or mutant EGFR was performed focusing on the significant gene. Results: Early growth response 1 (EGR1), a transcription factor, was the most strongly up-regulated gene in mutant EGFR-transfected cells among the genes examined. An increase in EGR1 expression in the mutant EGFR cells was confirmed using RT-PCR or immunoblotting. The expression was up-regulated by EGF stimulation and down-regulated by EGFR-tyrosine kinase inhibitor. In addition, the MEK inhibitor U0126 inhibited EGR1 expression, while the phosphatidylinositol 3-kinase inhibitor LY294002 did not. Conclusion: Mutant EGFR constitutively up-regulates EGR1 through the ERK pathway, and its expression is correlated with EGFR signal activation. Findings provide an insight into a target gene of mutant EGFR and further improve the understanding of the oncogenic properties of EGFR.*

Epidermal growth factor receptor (EGFR) is frequently overexpressed in various solid tumors (1, 2) and is regarded as a definitive oncogene. Accumulating data on EGFR and its signal pathway in cancer cells suggests that EGFR is a promising therapeutic target molecule; indeed, benefits from treatment with EGFR tyrosine kinase inhibitors (EGFR-TKIs) and anti-EGFR antibody have been confirmed in clinical settings (3, 4). Common *EGFR* mutations of DelE746_A750 and L858R, characterized by 15-base in-frame deletions or substitutions clustered around the ATP-binding site in exons 19 and 21 of *EGFR*, have been identified in patients with non-small cell lung cancer (NSCLC); these mutations are major determinants of sensitivity to EGFR-TKIs (5-8). Such mutations confer a constitutively active EGFR signal pathway to cancer cells (9).

The activated EGFR signal pathway has been intensively investigated, including studies on alterations in downstream signaling, the underlying mechanism responsible for sensitivity to EGFR-TKIs, the involvement in carcinogenesis, oncogene addiction, and clinico-pathological analyses. It has been previously reported that a lung cancer cell line, PC-9, with a deletional mutant of *EGFR* (delE746_A750) was hypersensitive to EGFR-TKIs and that this mutant *EGFR* was constitutively active and activated the ERK and AKT pathways (10-13). However, the changes in gene expression that occur in mutant *EGFR*-harboring cells have not been fully studied.

To identify changes in the gene expressions of downstream molecules that arise as a result of *EGFR* mutation and activated EGFR signaling, a microarray analysis of cells, in which the DelE746_A750-type of *EGFR* mutation had been stably introduced, was performed.

Materials and Methods

Reagents. The purified recombinant human EGF was purchased from R&D systems (Minneapolis, MN, USA). LY294002 2-(4-Morpholinyl)-8-phenyl-4H-benzopyran- 4-one was purchased from Calbiochem (San Diego, CA, USA), U0126 1,4-diamino-2,3-dicyano-1,4-bis[2-aminophenylthio] butadine was purchased from Cell Signaling Technology (Beverly, MA, USA).

Expression constructs and viral production. Full-length cDNA of wild-type *EGFR* was amplified by RT-PCR from a human embryonal kidney cell line (HEK293), and mutant *EGFR* (delE746_A750) was amplified from an NSCLC cell line (PC-9) (10, 14). Wild-type and mutant *EGFR* cDNA in a pcDNA3.1 vector (Clontech, Palo Alt, CA, USA) was cut out and introduced into a pQCLIN retroviral vector (BD Biosciences Clontech, San Diego, CA, USA) together with EGFP, followed by the internal ribosome entry sequence (IRES) to monitor the expression of the inserts indirectly. A pVSV-G vector (Clontech,

Correspondence to: Kazuto Nishio, Department of Genome Biology, Kinki University School of Medicine, 377-2 Ohno-higashi, Osaka-Sayama, Osaka 589-8511, Japan. Tel: +81 723676369, Fax: +81 723660206, e-mail: knishio@med.kindai.ac.jp

Key Words: EGFR, EGR1, microarray, mutation.

Palo Alt, CA, USA) for the constitution of the viral envelope and pQCXIX constructs were co-transfected into the GP2-293 cells using FuGENE6 transfection reagent. Briefly, 80% confluent cells cultured on a 10-cm dish were transfected with 2 μg of pVSV-G plus 6 μg of pQCXIX vectors. Forty-eight hours after transfection, the culture medium was collected and the viral particles were concentrated by centrifugation at 15,000 g for 3 h at 4°C. The viral pellet was then resuspended in fresh RPMI1640 medium. The titer of the viral vector was calculated by counting the EGFP-positive cells that were infected by serial dilutions of virus-containing medium, and the multiplicity of infection (MOI) was then determined.

Cell culture and transfection. The HEK293 cell line was cultured in DMEM (Sigma, St. Louis, MO, USA) supplemented with 10% fetal bovine serum (FBS), penicillin and streptomycin (Sigma) in a humidified atmosphere of 5% CO_2 at 37°C. The HEK293 cells were retrovirally transfected with the mock, wild-type and mutant *EGFR*, and the stable established cell lines were designated as HEK293-Mock, HEK293-Wild and HEK293-Del.

Real-time RT-PCR. One microgram of total RNA from a cultured cell line was converted to cDNA using a GeneAmp® RNA-PCR kit (Applied Biosystems, Foster City, CA, USA). Real-time PCR was carried out using the Applied Biosystems 7900HT Fast Real-time PCR System (Applied Biosystems) under the following conditions: 95°C for 6 min, and 40 cycles of 95°C for 15 sec and 60°C for 1 min. *GAPD* was used to normalize the expression levels in the subsequent quantitative analyses. To amplify the target genes, the following primers were purchased from TaKaRa (Yotsukaichi, Japan): EGR1-FW, GTA CAG TGT CTG TGC CAT GGA TTT C; EGR1-RW, GAG GAT CAC CAT TGG TTT GCT TG; GAPD-FW, GCA CCG TCA AGG CTG AGA AC; and GAPD-RW, ATG GTG GTG AAG ACG CCA GT. The results of three independent experiments were analyzed.

In vitro growth-inhibition assay. The growth-inhibitory effects of AG1478 (Biomol International, Plymouth Meeting, PA, USA) on the HEK293-Mock, -Wild and -Del cells were examined using an MTT assay. A 180-μL volume of an exponentially growing cell suspension (2×10^3 cells/well) was seeded into 96-well microtiter plates and 20 μL of various drug concentrations were added. After incubation for 72 h at 37°C, 20 μL of MTT solution (5 mg/mL in PBS) were added to each well and the plates were incubated for an additional 3 h at 37°C. After centrifuging the plates at 400 g for 5 min, the medium was aspirated from each well and 200 μL of DMSO was added to each well to dissolve the formazan. The optical density was measured at 570 nm. The results of three independent experiments were analyzed.

Immunoblotting. The antibodies used for immunoblotting were as follows: anti-EGFR (Upstate Biotechnology), anti-phospho-EGFR (Tyr1068), anti-p44/42 MAP kinase, anti-phospho-p44/42 MAP kinase, anti-Akt (Cell Signaling), anti-EGR1, anti-βactin (Santa Cruz), and anti-phospho-Akt (Ser473) (BD Bioscience, SanJose, CA, USA). Sub-confluent cells were washed with cold PBS and harvested with Lysis A buffer containing 1% Triton X-100, 20 mM Tris-HCl (pH 7.0), 5 mM EDTA, 50 mM sodium chloride, 10 mM sodium pyrophosphate, 50 mM sodium fluoride, 1 mM sodium orthovanadate, and a protease inhibitor mix, complete™ (Roche Diagnostics). Whole-cell lysates and the culture medium were separated using a 2-15% gradient SDS-PAGE and blotted onto a polyvinylidene fluoride membrane. After blocking with 3% bovine serum albumin in a TBS buffer (pH 8.0) with 0.1% Tween-20, the membrane was probed with primary antibody. After rinsing twice with TBS buffer, the membrane was incubated with horseradish peroxidase (HRP)-conjugated secondary antibody (Cell Signaling) and washed, followed by visualization using an ECL detection system (Amersham) and LAS-3000 (Fujifilm, Tokyo, Japan). The immunoblotting was performed in two independent experiments.

Microarray analysis. The microarray procedure was performed according to the Affymetrix protocols (Santa Clara, CA, USA). In brief, the total RNA extracted from the cell lines was analyzed using an Agilent 2100 Bioanalyzer (Agilent Technologies, Waldbronn, Germany) as a quality check, and cRNA was synthesized using the GeneChip® 3'-Amplification Reagents One-Cycle cDNA Synthesis Kit (Affymetrix). The labeled cRNAs were then purified and used to construct the probes. Hybridization was performed using the Affymetrix GeneChip HG-U133 Plus2.0 array for 16 h at 45°C. The signal intensities were measured using a GeneChip®Scanner3000 (Affymetrix) and converted to numerical data using the GeneChip Operating Software, Ver.1 (Affymetrix).

Statistical analysis. The microarray analysis was performed using the BRB Array Tools software ver. 3.3.0 (http://linus.nci.nih.gov/BRB-ArrayTools.html), developed by Dr. Richard Simon and Dr. Amy Peng. The microarray analysis was performed as described previously (15). Additional statistical analyses were performed using Microsoft Excel (Microsoft, Redmond, WA, USA) to calculate the standard deviation (SD) and statistically significant differences between each sample using the Student *t*-test. *P*-values of <0.05 were considered statistically significant.

Results

Early growth response 1 (EGR1) expression in mutant EGFR. The DelE746_A750-type *EGFR* mutation mediates a constitutively active EGFR signal and induces cellular hypersensitivity to EGFR-TKIs (11, 13). Mock, wild and mutant *EGFR* was introduced and stable cell lines was established as HEK293-Mock, -Wild and -Del cells. HEK293-Del cells showed increased phosphorylation levels of EGFR and ERK1/2 and were significantly hypersensitive to the EGFR-tyrosine kinase inhibitor AG1478, compared with the other cell lines (Figure 1A and 1B). To identify which gene expressions were changed by the *EGFR* mutation, a microarray analysis was performed for these stable cell lines. Twenty-three genes were identified as differentially expressed genes, the expressions of which differed by more than three-fold between HEK293-Wild and HEK293-Del cells (Table I). These genes included several cancer-related genes such as *EGR1, GALNT3, TACSTD1* (EpCAM), *MAFF, NLK, FOXN4, RUNX3* and *CD70*. Among them, *EGR1* was the most up-regulated gene in the HEK293-Del cells (>10-fold higher than in HEK293-Mock and -Wild cells, Figure 1C, 1D). The ratios of the signal intensity relative to that in the HEK293-Mock cells were 3.0-fold in the HEK293-Wild cells and 34.5-fold in the HEK293-Del

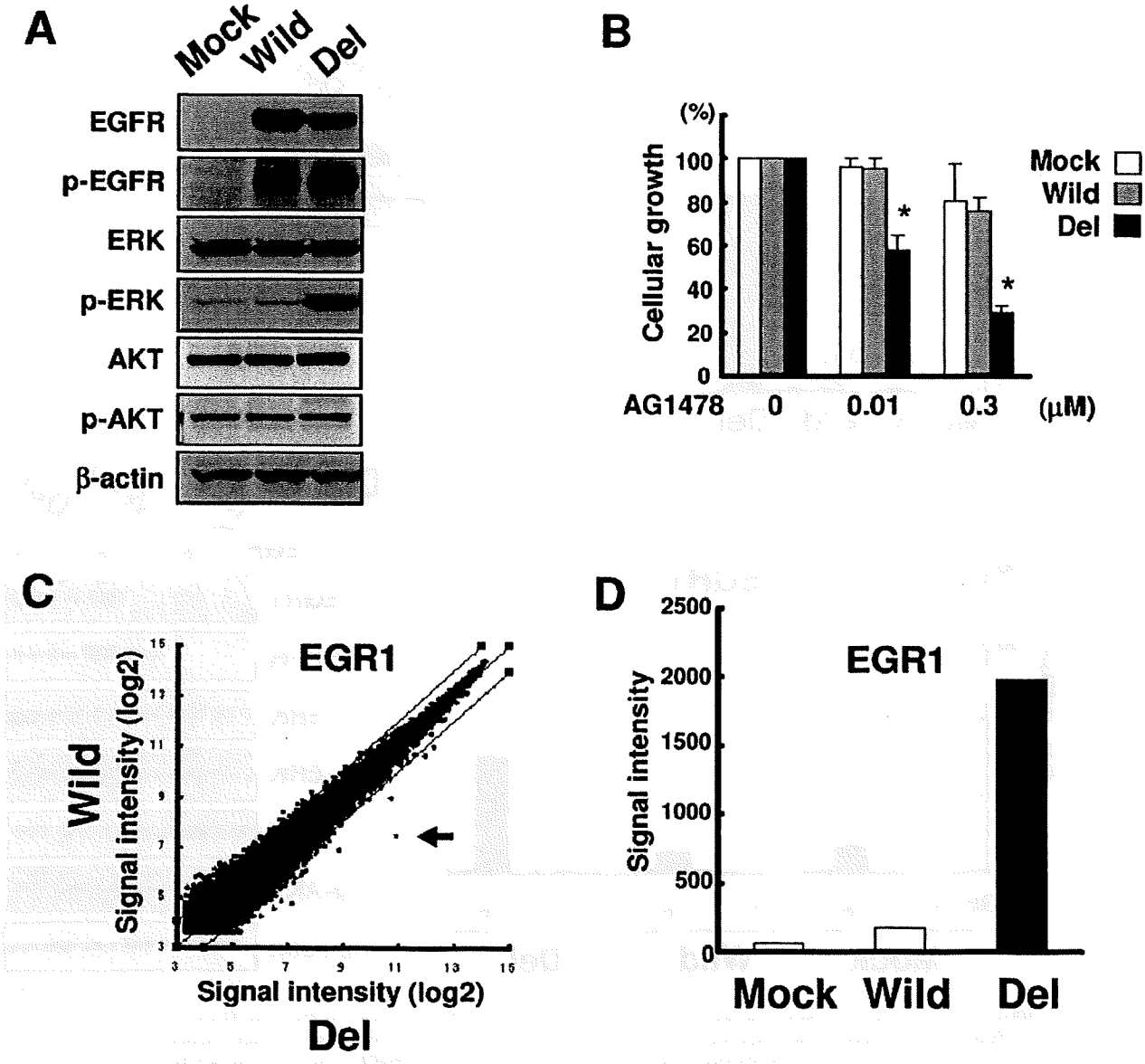

Figure 1. *Microarray analysis showing that mutant EGFR up-regulates EGR1 expression. (A) Immunoblotting for HEK293-Mock, -Wild and -Del cells cultured under normal conditions. The phosphorylation of EGFR and ERK1/2 was increased in HEK293-Del cells. (B) Growth inhibitory effect of an EGFR tyrosine kinase inhibitor. HEK293-Del cells were highly sensitive to AG1478. (C) Results of microarray analysis for genes with differential expressions between HEK293-Wild and -Del cells. The arrow indicates the EGR1 gene. (D) Signal intensity of microarray data for EGR1. EGR1 expression was up-regulated by more than 10-fold, compared with in HEK293-Wild cells. The error bars represent the SDs of three independent experiments. *: $p<0.05$.*

cells. Thus, the role of the *EGR1* transcription factor in EGFR signal activation was the focus of subsequent studies.

EGF stimulates EGR1 expression. The mRNA and protein levels of EGR1 up-regulation were confirmed using real-time RT-PCR and western blotting for these stable cell lines. Real-time RT-PCR revealed that *EGR1* mRNA expression in the HEK293-Wild cells was slightly (~3-fold) higher than that in the HEK293-Mock cells. On the other hand, *EGR1* mRNA expression was remarkably increased in the HEK293-Del cells (133-fold, compared with the HEK293-Mock cells). Similar results were obtained for the protein levels (Figure 2A, 2B). These results indicate that *EGR1* expression was constitutively up-regulated in the *EGFR* mutation-harboring cells.

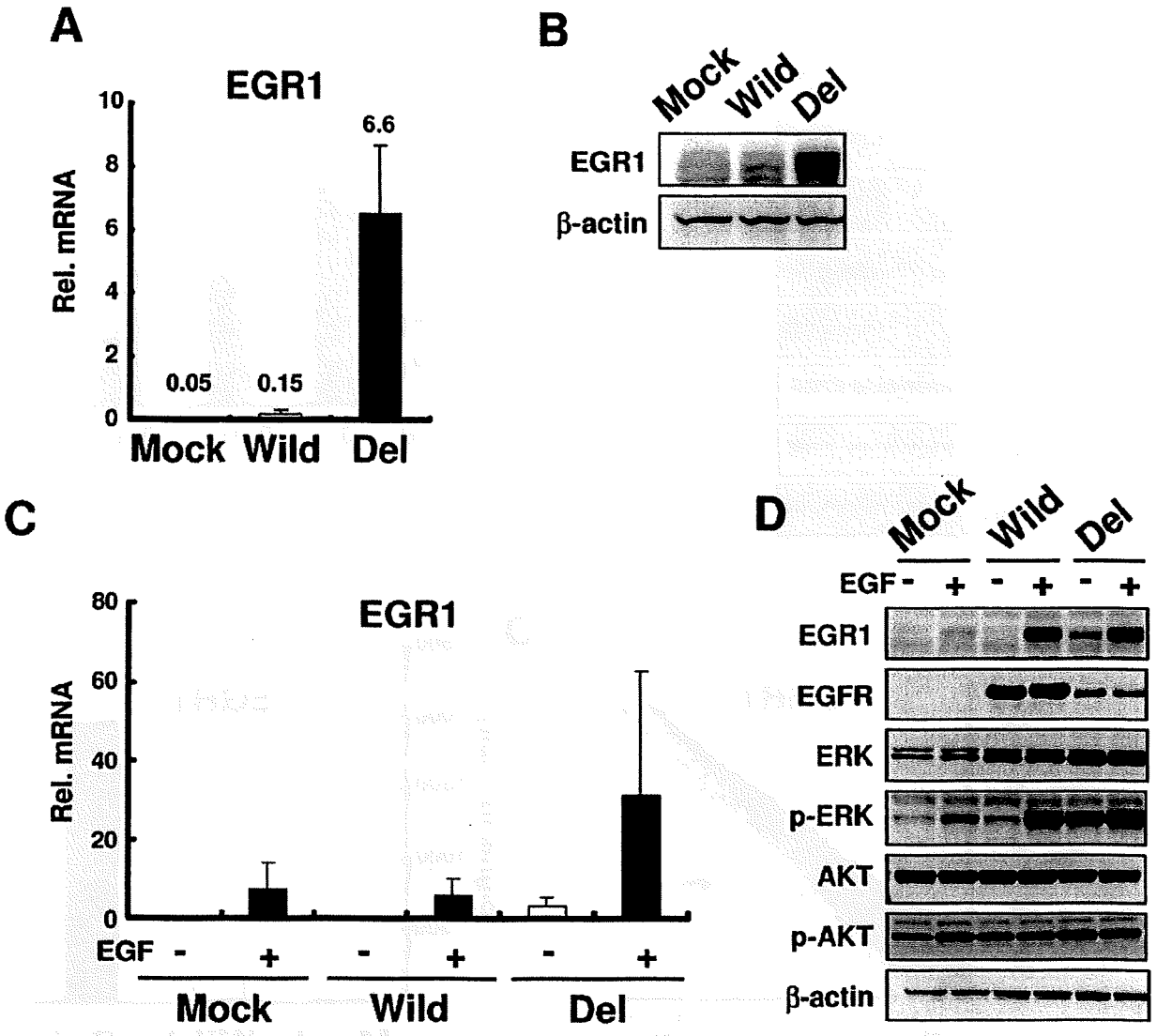

Figure 2. *Mutant EGFR up-regulates EGR1, and EGR1 expression is regulated by EGF stimulation. (A) Real-time RT-PCR shows that mutant EGFR up-regulates EGR1 by more than 40-fold, compared with in HEK293-Mock and -Wild cells cultured under normal conditions. (B) Immunoblotting shows the up-regulation of EGR1 in HEK293-Del cells. (C, D) EGF stimulation and EGR1 expression detected by real-time RT-PCR and immunoblotting. EGR1 expression was up-regulated by EGF, and the expression was correlated with the phospho-ERK1/2 levels. The error bars represent the SDs of three independent experiments. Immunoblotting was performed in two independent experiments. Rel. mRNA indicates the ratio of mRNA expression of EGR1/GAPD* $\times 10^{-6}$.

To examine whether the up-regulation of *EGR1* expression is regulated by EGFR signaling, the change in expression induced by EGF stimulation was evaluated. EGF increased *EGR1* mRNA expression in HEK293-Mock, -Wild and -Del cells (Figure. 2C). EGR1 up-regulation by EGF was also confirmed by immunoblotting (Figure 2D). HEK293-Wild cells stimulated with EGF expressed EGR1 to the same extent as in HEK293-Del cells, possibly reflecting the constitutively active function of EGFR in the HEK293-Del cells. In addition, EGR1 expression was closely correlated with the phospho-ERK1/2 expression levels. These findings suggest that EGR1 expression is involved in the ERK1/2 pathway.

EGFR-TKI down-regulates EGR1 expression. To elucidate the further relationship between *EGR1* up-regulation and EGFR signaling activity, the three cell lines were treated with EGFR-TKI. An EGFR-TKI, AG1478, inhibited the

Table I. *The results of microarray analysis for differentially expressed genes between HEK293-Wild and HEK293-Del cells. Twenty-three genes were identified as differentially expressed genes, the expressions of which differed by more than three-fold.*

Gene	Description	Probe set	Wild	Del	Fold change
EGR1	Early growth response 1	227404_s_at	172	1979	11.5
APOBEC3B	Apolipoprotein B mRNA editing enzyme	206632_s_at	27	147	5.4
GALNT3	UDP-N-acetyl-alpha-D-galactosamine	203397_s_at	118	477	4.1
TACSTD1	Tumor-associated calcium signal transducer 1	201839_s_at	23	91	3.9
MAFF	Transcription factor MAFF	36711_at	29	114	3.9
LOC646903	Hypothetical LOC646903	237116_at	19	67	3.6
UCHL1	Ubiquitin carboxyl-terminal esterase L1	201387_s_at	483	1733	3.6
RABL3	RAB, member of RAS oncogene family-like 3	226090_x_at	12	39	3.2
ZNF330	Zinc finger protein 330	213760_s_at	47	149	3.2
ERGIC2	ERGIC and golgi 2	226422_at	66	208	3.2
PHLDA2	Pleckstrin homology-like domain, family A, member 2	209803_s_at	59	183	3.1
TRIM5	Tripartite motif-containing 5	210705_s_at	13	40	3.1
KLHL23	Kelch-like 23 (Drosophila)	213610_s_at	62	192	3.1
C18orf37	Chromosome 18 open reading frame 37	1559716_at	56	13	0.23
NLK	Nemo-like kinase	238624_at	59	15	0.25
	CDNA FLJ34034 fis	238515_at	41	11	0.27
FOXN4	Forkhead box N4	241009_at	57	15	0.27
RUNX3	Runt-related transcription factor 3	204198_s_at	44	13	0.28
	transcribed locus	230746_s_at	70	21	0.31
CD70	CD70 molecule	206508_at	80	25	0.31
VDAC1	Voltage-dependent anion channel 1	217139_at	52	16	0.31
NBEA	Neurobeachin	226439_s_at	33	10	0.32
NID2	Nidogen 2 (osteonidogen)	204114_at	55	18	0.32

expression of both *EGR1* mRNA (Figure 3A) and protein (Figure 3B). EGR1 expression was also correlated with the phospho-ERK1/2 expression levels detected by immunoblotting. These results support the concept that EGR1 up-regulation by mutant EGFR is regulated by EGFR signaling.

EGR1 expression is regulated through the ERK1/2 pathway. EGR1 is thought to be a downstream molecule in the ERK1/2 pathway (16). To elucidate whether EGR1 up-regulation in mutant EGFR cells is regulated *via* the ERK1/2 pathway, ERK1/2 and AKT, two major downstream pathways of EGFR was evaluated. LY294002, a phosphatidylinositol 3-kinase inhibitor, inhibited the phosphorylation levels of AKT but did not modify the expression of EGR1 (Figure 4A). However, the MEK inhibitor U0126 clearly down-regulated EGR1 expression in HEK293-Del cells (Figure 4B). EGR1 expression was consistent with the phospho-ERK1/2 expression levels. These results strongly suggest that EGR1 up-regulation by mutant *EGFR* is regulated through the ERK pathway. Based on these findings, a model was propossed to explain the up-regulation of EGR1 by mutant *EGFR* (Figure 4C). In this model, mutant *EGFR* activates the ERK pathway and induces *EGR1* transcription.

Discussion

EGR1 transcription factor is induced by various stimuli, including growth factors, hypoxia, UV and cytokines, and mediates multiple cellular responses such as mitogenesis, differentiation, cellular survival, anti-apoptosis, angiogenesis and apoptosis (17). In cancer biology, *EGR1* is basically regarded as a tumor suppressor gene because it directly regulates p53, PTEN and TGFβ1. Deletion of the *EGR1*-containing 5q31 region has been associated with a certain type of lymphoma and small cell lung carcinoma. Low EGR1 expression in tumor tissue is frequently observed in breast cancer, glioblastoma and other solid tumors (18). In contrast, the oncogenic property of *EGR1* is observed in prostate cancer (19).

An increased expression of *EGR1* was observed in mutant *EGFR* cells. Previous reports have demonstrated that mutant *EGFR* is oncogenic in non-small cell lung cancer (20). However, Ferraro *et al.* have demonstrated that *EGR1* expression is strongly correlated with PTEN expression and that patients with high levels of EGR1 had better overall and disease-free survival periods than patients with low levels of EGR1 in patients with NSCLC (21). It was speculated that the overexpression of EGR1 in mutant *EGFR* cells may play some role in the biological behaviors of mutant *EGFR* in cancer.

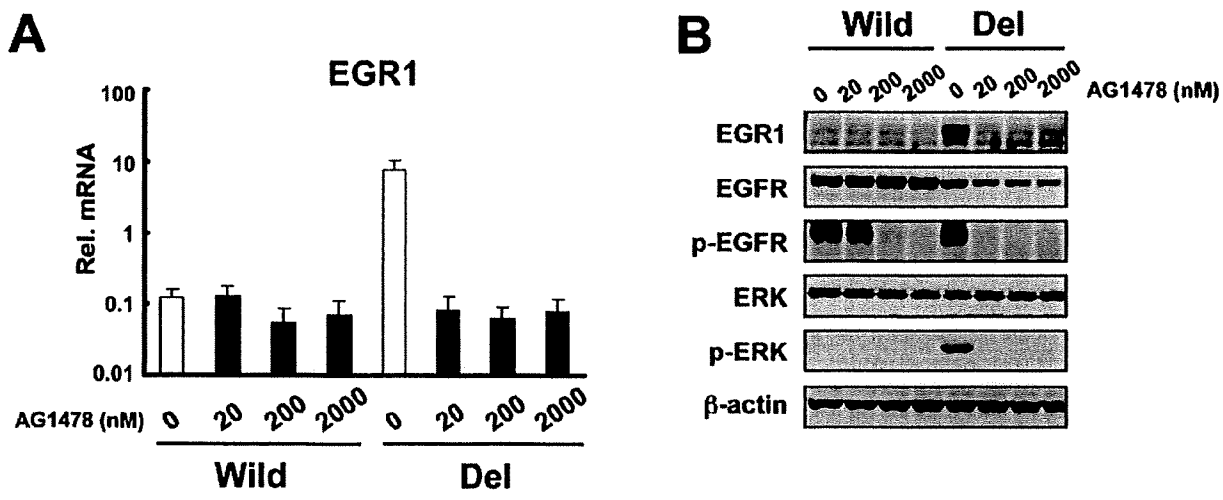

Figure 3. *EGFR tyrosine kinase inhibitor down-regulates EGR1 expression. (A) Real-time RT-PCR and (B) immunoblotting were performed for cells cultured under normal conditions and treated with four concentrations of AG1478 for 5 h. EGFR tyrosine kinase inhibitor clearly down-regulated EGR1 expression. The phosphorylation levels of EGFR decreased at a lower concentration (20 nM) in HEK293-Del cells than in HEK293-Wild cells. Note that the Y-axis is a log-scale. Error bars represent the SDs of three independent experiments. Immunoblotting was performed in two independent experiments. Rel. mRNA indicates the ratio of mRNA expression of EGR1/GAPD × 10^{-6}.*

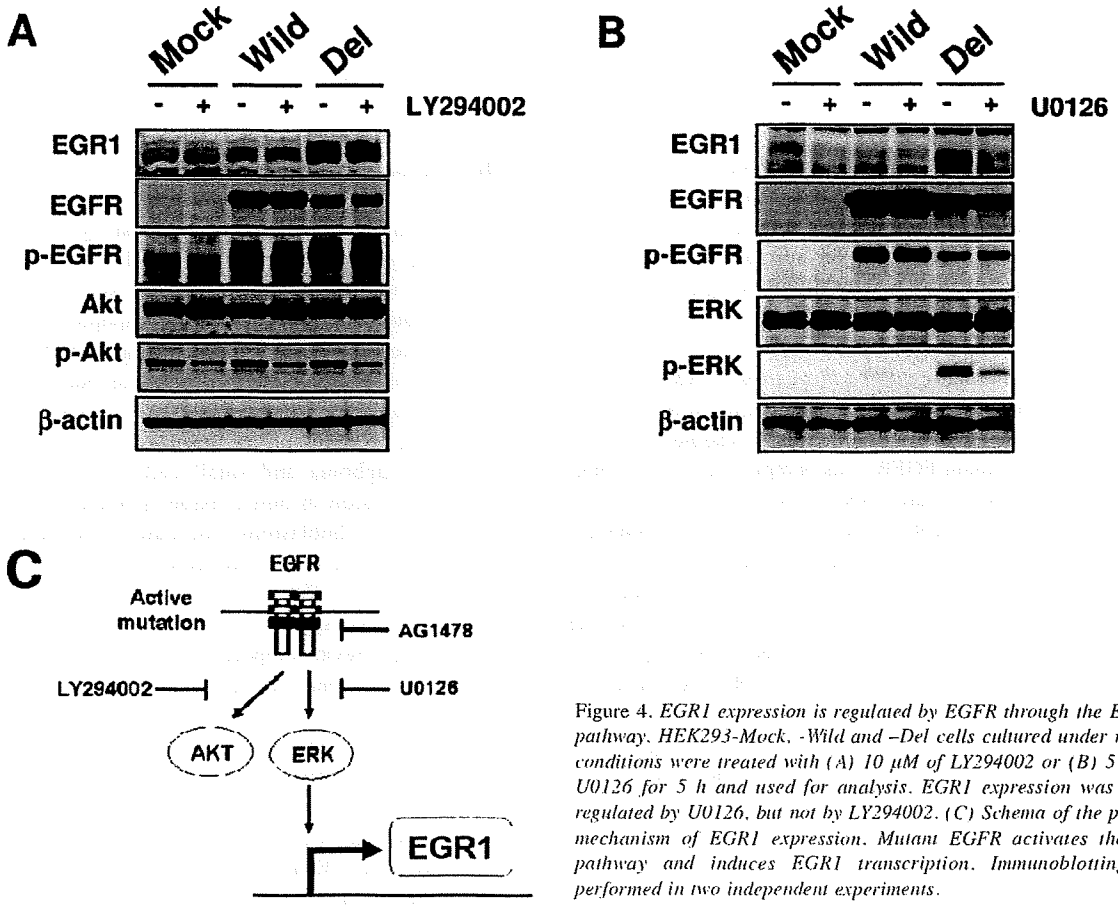

Figure 4. *EGR1 expression is regulated by EGFR through the ERK1/2 pathway. HEK293-Mock, -Wild and -Del cells cultured under normal conditions were treated with (A) 10 μM of LY294002 or (B) 5 μM of U0126 for 5 h and used for analysis. EGR1 expression was down-regulated by U0126, but not by LY294002. (C) Schema of the putative mechanism of EGR1 expression. Mutant EGFR activates the ERK pathway and induces EGR1 transcription. Immunoblotting was performed in two independent experiments.*

In general, ERK and JNK kinases phosphorylate ternary complex factors (TCF), which cooperate with serum response factor (SRF) to induce *EGR1* transcription in vascular biology (22). *EGR1* can displace Sp1 and other transcription factors, and EGR1 transactivation leads to the transcription of many EGR1-target genes. To date, several putative EGR1-target genes related to cancer have been identified, including cyclin D, EGFR, FGF, IGF-I, thymidine kinase, PDGF-A, Bcl2, CD44, p53, PTEN, TNF-α and VEGF. Further investigation of the biological role of EGR1 overexpression in mutant *EGFR* may lead to a better understanding of the roles of mutant *EGFR* in cancer cells.

In conclusion, it was found that mutant *EGFR* induced EGR1 overexpression and that this overexpression was correlated with EGFR signal activation through ERK1/2. These results provide a novel insight into the oncogenic properties of EGFR in cancer cells.

Acknowledgements

This work was supported by funds for the Third-Term Comprehensive 10-Year Strategy for Cancer Control and the program for the promotion of Fundamental Studies in Health Sciences of the National Institute of Biomedical Innovation (NiBio) and the Japan Health Sciences Foundation.

We thank Dr. Richard Simon and Dr. Amy Peng for providing the BRB ArrayTools software.

References

1 Cowley GP, Smith JA and Gusterson BA: Increased EGF receptors on human squamous carcinoma cell lines. Br J Cancer *53*: 223-229, 1986.

2 Gusterson B, Cowley G, McIlhinney J, Ozanne B, Fisher C and Reeves B: Evidence for increased epidermal growth factor receptors in human sarcomas. Int J Cancer *36*: 689-693, 1985.

3 Karamouzis MV, Grandis JR and Argiris A: Therapies directed against epidermal growth factor receptor in aerodigestive carcinomas. JAMA *298*: 70-82, 2007.

4 Rocha-Lima CM, Soares HP, Raez LE and Singal R: EGFR targeting of solid tumors. Cancer Control *14*: 295-304, 2007.

5 Mitsudomi T, Kosaka T, Endoh H *et al*: Mutations of the epidermal growth factor receptor gene predict prolonged survival after gefitinib treatment in patients with non-small-cell lung cancer with postoperative recurrence. J Clin Oncol *23*: 2513-2520, 2005.

6 Paez JG, Janne PA, Lee JC *et al*: EGFR mutations in lung cancer: correlation with clinical response to gefitinib therapy. Science *304*: 1497-1500, 2004.

7 Pao W, Miller V, Zakowski M *et al*: EGF receptor gene mutations are common in lung cancers from "never smokers" and are associated with sensitivity of tumors to gefitinib and erlotinib. Proc Natl Acad Sci USA *101*: 13306-13311, 2004.

8 Tokumo M, Toyooka S, Kiura K *et al*: The relationship between epidermal growth factor receptor mutations and clinicopathologic features in non-small cell lung cancers. Clin Cancer Res *11*: 1167-1173, 2005.

9 Amann J, Kalyankrishna S, Massion PP *et al*: Aberrant epidermal growth factor receptor signaling and enhanced sensitivity to EGFR inhibitors in lung cancer. Cancer Res *65*: 226-235, 2005.

10 Arao T, Fukumoto H, Takeda M, Tamura T, Saijo N and Nishio K: Small in-frame deletion in the epidermal growth factor receptor as a target for ZD6474. Cancer Res *64*: 9101-9104, 2004.

11 Koizumi F, Shimoyama T, Taguchi F, Saijo N and Nishio K: Establishment of a human non-small cell lung cancer cell line resistant to gefitinib. Int J Cancer *116*: 36-44, 2005.

12 Sakai K, Arao T, Shimoyama T *et al*: Dimerization and the signal transduction pathway of a small in-frame deletion in the epidermal growth factor receptor. FASEB J *20*: 311-313, 2006.

13 Sakai K, Yokote H, Murakami-Murofushi K, Tamura T, Saijo N and Nishio K: In-frame deletion in the EGF receptor alters kinase inhibition by gefitinib. Biochem J *397*: 537-543, 2006.

14 Matsumoto K, Yokote H, Arao T *et al*: N-Glycan fucosylation of epidermal growth factor receptor modulates receptor activity and sensitivity to epidermal growth factor receptor tyrosine kinase inhibitor. Cancer Sci *99*: 1611-1617, 2008.

15 Igarashi T, Izumi H, Uchiumi T *et al*: Clock and ATF4 transcription system regulates drug resistance in human cancer cell lines. Oncogene *26*: 4749-4760, 2007.

16 Lo LW, Cheng JJ, Chiu JJ, Wung BS, Liu YC and Wang DL: Endothelial exposure to hypoxia induces Egr-1 expression involving PKCalpha-mediated Ras/Raf-1/ERK1/2 pathway. J Cell Physiol *188*: 304-312, 2001.

17 Adamson ED and Mercola D: Egr1 transcription factor: multiple roles in prostate tumor cell growth and survival. Tumour Biol *23*: 93-102, 2002.

18 Baron V, Adamson ED, Calogero A, Ragona G and Mercola D: The transcription factor Egr1 is a direct regulator of multiple tumor suppressors including TGFbeta1, PTEN, p53, and fibronectin. Cancer Gene Ther *13*: 115-124, 2006.

19 Adamson E, de Belle I, Mittal S *et al*: Egr1 signaling in prostate cancer. Cancer Biol Ther *2*: 617-622, 2003.

20 Lynch TJ, Bell DW, Sordella R *et al*: Activating mutations in the epidermal growth factor receptor underlying responsiveness of non-small-cell lung cancer to gefitinib. N Engl J Med *350*: 2129-2139, 2004.

21 Ferraro B, Bepler G, Sharma S, Cantor A and Haura EB: EGR1 predicts PTEN and survival in patients with non-small-cell lung cancer. J Clin Oncol *23*: 1921-1926, 2005.

22 Silverman ES and Collins T: Pathways of Egr-1-mediated gene transcription in vascular biology. Am J Pathol *154*: 665-670, 1999.

Received October 20, 2008
Revised January 19, 2009
Accepted February 13, 2009

research articles Journal of proteome research

Identification of Predictive Biomarkers for Response to Trastuzumab Using Plasma FUCA Activity and N-Glycan Identified by MALDI-TOF-MS

Kazuko Matsumoto,[†,§,#] Chikako Shimizu,[‡,#] Tokuzo Arao,[†] Masashi Andoh,[‡] Noriyuki Katsumata,[‡] Tsutomu Kohno,[‡] Kan Yonemori,[‡] Fumiaki Koizumi,[||] Hideyuki Yokote,[†] Kenjiro Aogi,[⊥] Kenji Tamura,[‡] Kazuto Nishio,[*,†] and Yasuhiro Fujiwara[‡]

Department of Genome Biology, Kinki University School of Medicine, Osaka, Japan, Medical Oncology, National Cancer Center Hospital, Tokyo, Japan, First Department of Internal Medicine, Osaka Medical College, Osaka, Japan, Shien Lab, National Cancer Center Hospital, Tokyo, Japan, and Department of Surgery, National Hospital Organization Shikoku Cancer Center, Matsuyama, Japan

Received August 19, 2008

The aim of this study was to identify glycobiological biomarkers that indicate sensitivity to trastuzumab, a humanized monoclonal antibody against HER2 in plasma samples from breast cancer patients. Plasma samples were obtained from 24 breast cancer patients treated with trastuzumab monotherapy. The catalytic activities of plasma α1-6, fucosyltransferase (FUT8) and α-L fucosidase (FUCA) were analyzed using high-performance liquid chromatography (HPLC) and spectrophotometer, respectively. The plasma N-glycan profiles were investigated using matrix-assisted laser desorption/ionization time-of-flight mass spectrometry (MALDI-TOF-MS). Plasma FUT8 activity was not significantly correlated with either the clinical response or progression-free survival (PFS). On the other hand, plasma FUCA activity was significantly correlated with PFS ($p < 0.05$). The MALDI-TOF-MS analysis of the plasma N-glycan profile revealed that the expression of 2534 *m/z* N-glycan was lower in patients with progressive disease (PD) and was correlated with PFS. Low expression of 2534 *m/z* N-glycan discriminated between PD and non-PD with 75% sensitivity and 82% specificity. We demonstrated that the plasma FUCA activity and 2534 *m/z* N-glycan may be predictive biomarkers of sensitivity to trastuzumab. Our results suggest that glycosylation analysis may provide useful information for determining clinical cancer therapy and provide novel insight into biomarker studies using glycobiological tools in the field of breast cancer.

Keywords: FUT8 • FUCA • N-glycan • trastuzumab • breast cancer

Introduction

The glycosylation of proteins is an important post-translational modification that plays a critical role in cancer biology including cellular growth, differentiation, adhesion and metastasis.[1−4] Specific carbohydrate chains and glycosyltransferase are associated with the biological functions of cancer cells.[5,6] Recently, many researchers have evaluated the use of glycosylated proteins, such as carbohydrate antigens CA19−9 and CA125, as biomarkers for early diagnosis or tumor progression.[7−9]

The fucosylation of N-linked oligosaccharides is one of the most important glycosylation events in biological function, including cancer.[10,11] For example, fucosylated α-fetoprotein is a highly specific tumor marker of hepatocellular carcinoma.[12] α1-6, Fucosyltransferase (FUT8) is known to transfer a fucose residue to N-linked oligosaccharides on glycoproteins.[13] A series of studies have demonstrated that nonfucosylated antibody, which is produced by the knockout of the FUT8 gene, enhances antibody-dependent cellular cytotoxicity (ADCC) and the cytotoxic effect of the antibody.[14−16] These results indicate that FUT8 plays an important role in ADCC activity. α-L fucosidase (FUCA), on the other hand, is a lysosomal hydrolase that has been identified in tissues and serum. Serum FUCA activity is reportedly correlated with early detection in hepatocellular carcinoma[17] and may be a useful prognostic marker and a predictive marker of tumor recurrence in colorectal cancer.[18,19]

HER2 (also known as NEU, EGFR2, or ERBB2) is a member of the epidermal growth factor receptor (EGFR) family. HER2 is amplified in 25−30% of human primary breast cancers and predicts a poor prognosis.[20−22] Trastuzumab (Herceptin; Roche, Basel, Switzerland), a humanized monoclonal antibody against HER2, is a potent anticancer agent that is used in standard chemotherapy against HER2-overexpressing breast cancer in

* To whom correspondence should be addressed. Kazuto Nishio, Department of Genome Biology, Kinki University School of Medicine, 377-2 Ohno-Higashi, Osaka-Sayama, Osaka, Japan. Tel: +81-72-366-0221. Fax: +81-72-366-0206. E-mail: knishio@med.kindai.ac.jp.
† Kinki University School of Medicine.
§ Osaka Medical College.
‡ Medical Oncology, National Cancer Center Hospital.
# These authors contributed equally to this work.
|| Shien Lab, National Cancer Center Hospital.
⊥ National Hospital Organization Shikoku Cancer Center.

10.1021/pr800655p CCC: $40.75

Published on Web 01/13/2009

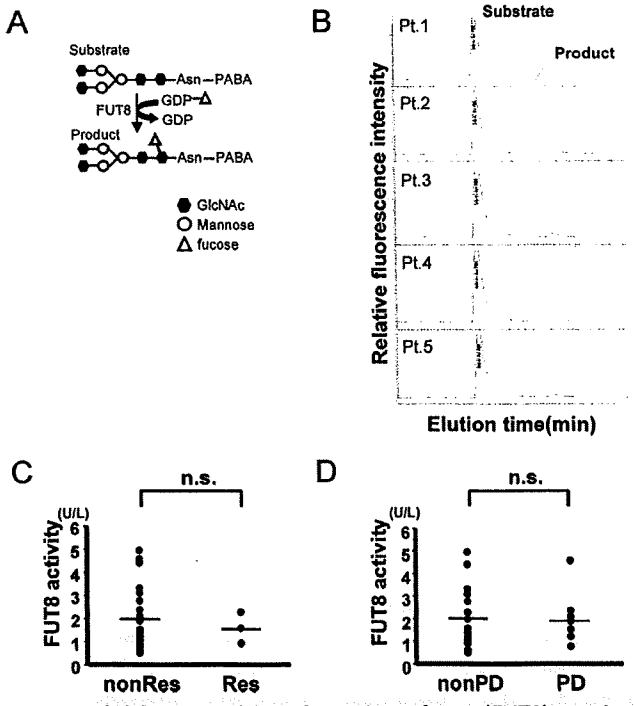

Figure 1. (A) Schema of α1-6, fucosyltransferase (FUT8) reaction used to measure FUT8 enzymatic activity. Asn, asparagine; PABA, 4-(2-pyridylamino) butylamine. (B) HPLC data for plasma FUT8 activities in clinical samples. The substrate (GnGn-bi-Asn-PABA) is fucosylated by FUT8 and detected as the product. FUT8 activity is measured using HPLC. The enzyme activities were analyzed in duplicate. (C) Plasma FUT8 activity and clinical response. Res, responder group (complete response + partial response); non-Res, nonresponder group (stable disease + progressive disease). n.s.: not significant. (D) Plasma FUT8 activity and clinical response. PD, progressive disease group; nonPD, nonprogressive disease group. n.s.: not significant.

combination with other chemotherapeutic agents.[23,24] In some patients with HER2 overexpression, however, trastuzumab dose not have any anticancer effect. In addition, trastuzumab can induce severe adverse effects, such as cardiac dysfunction.

Therefore, biomarkers are needed to predict the clinical outcome of trastuzumab therapy in patients with breast cancer. We previously reported that trastuzumab-induced ADCC is a major mechanism of action,[25] in addition to the effects of anti-EGFR antibody.[26] We have also identified a sensitivity determinant factor for EGFR-targeting drugs[27,28] and recently demonstrated that FUT8 regulated the fucosylation level of EGFR and modifies EGF-mediated cellular growth and sensitivity to EGFR tyrosine kinase inhibitor.[29]

In the present study, we attempted to identify predictive biomarkers of sensitivity to trastuzumab, focusing on fucosylation and glycosylation. For this purpose, plasma FUT8 and FUCA activity and the N-glycan profiles were examined in breast cancer patients treated with trastuzumab monotherapy.

Materials and Methods

Patients and Blood Samples. This prospective study was started in August 2005 and enrollment at the National Cancer Center Hospital and Shikoku Cancer Center Hospital was completed in August 2007. Eligible patients had histologically confirmed, nonlife-threatinig, postoperative recurrent or stage IV HER2-positive breast cancer, and were intended to receive trastuzumab monotherapy. The HER2 status was confirmed using immunohistochemistry (IHC) 3+ or fluorescence in situ hybridization (FISH)-positive utilizing core needle biopsy (CNB) samples of the tumor tissue. All the patients were treated with trastuzumab (4 mg/kg on day 1 and thereafter at a dose of 2 mg/kg weekly), and 24 patients were evaluated. The response to trastuzumab therapy was evaluated based on a CT scan, magnetic resonance imaging (MRI) or ultrasound examination of the tumor before and 8 weeks after treatment and was classified according to the Response Evaluation Criteria in Solid Tumors. Plasma samples were obtained immediately before trastuzumab treatment, centrifuged and stored at −80 °C. The study was approved by the Institutional Review Boards of the National Cancer Center Hospital, Kinki University Hospital and Shikoku Cancer Center Hospital, and written informed consent was obtained from all the patients.

Table 1. Clinical Characteristics of Study Population[a]

characteristics		no. of patients	%
Age	Mean	60	
	Range	28–76	
Prior chemotherapy	Present	17	71
	Absent	6	25
	ND	1	4
Prior radiotherapy	Present	14	58
	Absent	9	38
	ND	1	4
PS	0	8	33
	1	15	63
	2	1	4
Metastasis	Lung	15	63
	Liver	3	13
	Bone	5	21
	Brain	2	8
	LN	10	42
	Others	2	8
Hormone receptor	ER (+)	12	50
	ER (−)	12	50
	PgR (+)	11	46
	PgR (−)	12	50
	ND	1	4

[a] ND, not determined; PS, performance status; ER, estrogen receptor; PgR, progesterone receptor.

FUT8 Activity Assay. The method used to perform the FUT8 activity assay has been previously described.[30] Briefly, the fluorescent substrate (GnGn-bi-Asn-PABA, Figure 1A) was purchased from Peptide Institute, Inc. (Osaka, Japan). The standard mixture for measuring FUT8 activity contained 50 μM of substrate, 200 mM of MES (pH 7.0), 1% Triton X, 500 μM of GDP-Fucose and 23 μL of the plasma sample in a final volume of 50 μL. The reaction mixture was incubated at 37 °C for 6 h, and the reaction was stopped by heating at 100 °C for 1 min. The sample was then centrifuged at 15 000*g* for 10 min, and the supernatant (5 μL) was used for the analysis. The product was separated using high-performance liquid chromatography (HPLC) with a TSK-gel ODS-80TM column (4.6 × 150 mm). Elution was performed at 55 °C with a 20 mM acetate buffer, pH 4.0, containing 0.1% butanol. The fluorescence of the column elute was detected using a fluorescence photometer (HITACHI Fluorescence Spectrophotometer 650−10LC). The excitation and emission wavelengths were observed at 320 and 400 nm, respectively. The product area was used to calculate the enzyme activity (U/L) in all the patients. The enzyme activities were analyzed in duplicate.

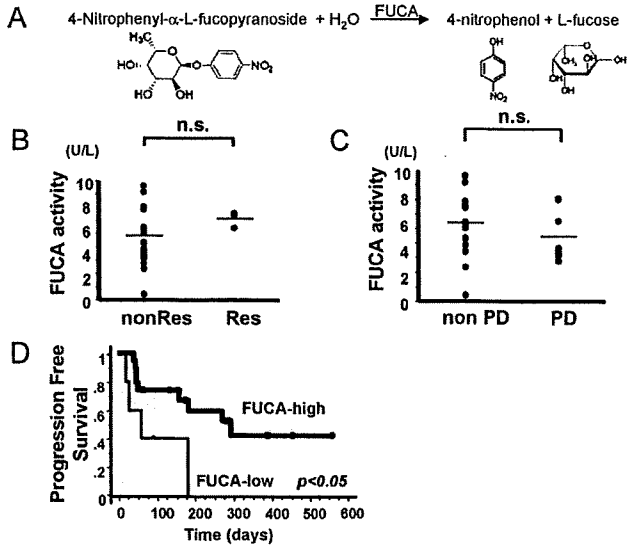

Figure 2. (A) Reaction pathway of α-L fucosidase (FUCA) activity. The substrate (4-nitrophenyl-α-L-fucopyranoside) is defucosylated by FUCA and the products are detected. FUCA activity is measured using spectrophotometer. The enzyme activities were analyzed in duplicate. (B) Plasma FUCA activity and clinical response. Res, responder group (complete response + partial response); nonRes, nonresponder group (stable disease + progressive disease). n.s.: not significant. (C) Plasma FUCA activity and clinical response. PD, progressive disease group; nonPD, nonprogressive disease group. n.s.: not significant. (D) Kaplan–Meier curve for progression-free survival (PFS) of trastuzumab treatment. Patients with a high plasma FUCA activity (4.3 > U/L) exhibited a significantly prolonged PFS ($p < 0.05$).

FUCA Activity Assay. The standard mixture for measuring α-L fucosidase activity contained 20 μL of the plasma sample, 2 mM of 4-nitrophenyl-α-L-fucopyranoside (Sigma, St. Louis, MO), and 50 mM of citrate buffer (pH 4.5) in a final volume of 150 μL in a 96-well microplate. The mixture was incubated at 37 °C for 3 h, and the reaction was stopped by the addition of 100 μL of 0.4 M borate buffer (pH 9.8). The optical density was measured at 405 nm. One unit of enzyme was defined as the amount of enzyme required to produce 1 mmol of product per minute at 37 °C. The enzyme activities were analyzed in duplicate.

Purification of Plasma N-Glycan. Twenty-seven microliters of plasma sample was dissolved in 83 mM ammonium bicarbonate and 10 mM DL-dithiothreitol (Sigma-Aldrich, St. Louis, MO) in a final volume of 60 μL. The mixture was incubated at 60 °C for 30 min, and 10 μL of 123 mM iodoacetamide (Wako Pure Chemicals Co., Tokyo, Japan) was added. After incubation for 1 h at room temperature in the dark, 400 units of trypsin (Sigma-Aldrich) was added to the mixture. The mixture was incubated at 37 °C for 2 h, and the reaction was stopped by heating at 90 °C for 5 min. Five units of peptide *N*-glycosidase F (Roche Diagnostics, Mannheim, Germany) was added, and the mixture was incubated at 37 °C overnight. The internal standard (mannononaose-di-(*N*-acetyl-D-glucosamine), Sigma-Aldrich) was added, and N-glycan was purified from the mixture using BlotGlyco (Sumitomo Bakelite, Co., Tokyo, Japan) according to the manufacture's protocol.[31]

Mass Spectrometry Analysis. The purified samples were concentrated, and 0.5 μL of the sample solution was applied to a sample plate target, then mixed with 0.5 μL of the matrix solution. 2, 5-Dihydroxybenzoic acid (Aldrich) was dissolved in 50% acetonitrile using the matrix solution. After the samples had dried, MALDI-TOF-MS was performed using a Voyager-DE STR Workstation (Applied Biosystems) in reflector, positive ion mode. The number of laser shots was 300 × 2 shots and the mass range acquired was 700–5000 Da. The N-glycan structure was achieved using the GlycoSuite online database, proteome System. The MALDI-TOF-MS spectra data was exported using Voyager Biospectrometry Workstation ver 5.1, Data Explorer Software (Applied Biosystem).

Statistical Analysis. The statistical analyses of the enzyme activity assays and the clinical outcome were performed using the Student's *t*-test by StatView version 5 software (SAS Institute, Inc., Cary, NC). Progression-free survival curves were estimated using the Kaplan–Meier method (StatView). All plasma N-glycans peaks obtained from MALDI-TOF-MS were normalized using an internal standard (mannononaose-di-(*N*-acetyl-D-glucosamine)). The normalized data was imported into BRB Array Tools software ver. 3.3.0 (http://linus.nci.nih.gov/BRB-ArrayTools.html), developed by Dr. Richard Simon and Dr. Amy Peng. N-Glycan peaks were selected for analysis if the peak was observed in over 50% of the patients (>12 patients); finally, 31 peaks of N-glycan were selected. A statistical analysis comparing the N-glycan peaks to response to treatment or PFS was performed. A *p*-value of <0.05 was considered significant.

Result

Patient Characteristics. Twenty-four patients were evaluated in this study. The mean patient age was 60 years (range 28–76 years). Seventy-one percent (17/24 pts) of the patients had received prior adjuvant chemotherapy, and 58% (14/24 pts) of the patients had received prior radiotherapy. Almost all the patients had a performance status (PS) of 0 or 1 (23/24 pts), and the metastatic sites and hormone receptor status were shown (Table 1). Table 1 summarizes the clinical features of the patients.

Plasma FUT8 Activity and Clinical Outcome. Plasma FUT8 activity was measured using reverse-phase HPLC with a fluorescent substrate (Figure 1A). A representative elution pattern of FUT8 activity in the plasma sample is shown in Figure 1B. The elution times of the substrate and product were 15 and 27 min, respectively. The product area was calculated to determined the overall catalytic activity. The average FUT8 enzyme activity was 2.0 ± 1.3 U/L (average ± SD; range, 0.5 to 5.0 U/L). Regarding the clinical outcome, the FUT8 catalytic activities of responders (CR, complete response; PR, partial response, $n = 3$) and nonresponders (SD, stable disease; PD, progressive disease, $n = 21$) were 1.6 ± 0.7 U/L and 2.0 ± 1.4 U/L, respectively. The activities of the PD and non-PD groups were 1.9 ± 1.2 U/L and 2.0 ± 1.4 U/L, respectivily. No significant correlations between FUT8 activity and the clinical response to trastuzumab were seen (Figure 1C,D). Also, no significant correlations were seen between FUT8 activity and progression-free survival (PFS, data not shown). These results suggest that plasma FUT8 activity is not a useful biomarker for this population.

Correlation of Plasma FUCA Activity and PFS. Plasma FUCA activity was examined using spectrophotometer and 4-nitrophenyl-α-L-fucopyranoside (Figure 2A). The average FUCA enzyme activity was 6.1 ± 2.1 U/L (average ± SD; range, 1.5 to 9.7 U/L). The activities of responders, nonresponders, the PD group and the non-PD group were 7.2 ± 0.6, 5.9 ± 2.2, 5.5 ± 1.8 and 6.3 ± 2.2 U/L, respectively. No significant correlations between FUCA activity and the clinical response to trastuzumab

Table 2. List of Predominant Oligosaccharides in Patient Serum Samples[a]

measured MS (*m/z*)	putative structure
1286.6	ND
1300.6	(Hex)2 (HexNAc)2 (Deoxyhexose)2
1495.5	(Hex)2 + (Man)3(GlcNAc)2
1657.6	(Hex)3 + (Man)3(GlcNAc)2
1701.6	ND
1723.7	(HexNAc)2 (Deoxyhexose)1 + (Man)3(GlcNAc)2
1739.7	(Hex)1 (HexNAc)2 + (Man)3(GlcNAc)2
1841.7	(Hex)1 (HexNAc)1 (NeuAc)1 + (Man)3(GlcNAc)2
1885.7	(Hex)1 (HexNAc)2 (Deoxyhexose)1 + (Man)3(GlcNAc)2
1901.7	(Hex)2 (HexNAc)2 + (Man)3(GlcNAc)2
1926.7	(HexNAc)3 (Deoxyhexose)1 + (Man)3(GlcNAc)2
2047.8	(Hex)2 (HexNAc)2 (Deoxyhexose)1 + (Man)3(GlcNAc)2
2088.8	(Hex)1 (HexNAc)3 (Deoxyhexose)1 + (Man)3(GlcNAc)2
2121.8	(Hex)1 (HexNAc)1 (Deoxyhexose)4 + (Man)3(GlcNAc)2
2206.8	(Hex)2 (HexNAc)2 (NeuAc)1 + (Man)3(GlcNAc)2
2220.8	(HexNAc)3 (Deoxyhexose)3 + (Man)3(GlcNAc)2
2352.9	(Hex)2 (HexNAc)2 (Deoxyhexose)1 (NeuAc)1 + (Man)3(GlcNAc)2
2489.9	(Hex)5 (HexNAc)1 (NeuAc)1 + (Man)3(GlcNAc)2
2493.9	(Hex)1 (HexNAc)5 (Deoxyhexose)1 + (Man)3(GlcNAc)2
2497.9	(Hex)2 (HexNAc)2 (Deoxyhexose)2 (NeuAc)1 + (Man)3(GlcNAc)2
2511.9	(Hex)2 (HexNAc)2 (NeuAc)2 + (Man)3(GlcNAc)2
2519.9	(Hex)4 (HexNAc)2 (Deoxyhexose)2 + (Man)3(GlcNAc)2
2527.9	(Hex)1 (HexNAc)3 (Deoxyhexose)4 + (Man)3(GlcNAc)2
2533.9	(Hex)5 (HexNAc)2 (Deoxyhexose)1 + (Man)3(GlcNAc)2 (Hex)3 (Deoxyhexose)6 + (Man)3(GlcNAc)2
2556.0	(Hex)2 (HexNAc)3 (Deoxyhexose)1 (NeuAc)1 + (Man)3(GlcNAc)2
2572.0	(Hex)3 (HexNAc)3 (NeuAc)1 + (Man)3(GlcNAc)2
2658.0	(Hex)2 (HexNAc)2 (Deoxyhexose)1 (NeuAc)2 + (Man)3(GlcNAc)2
2748.0	(Hex)2 (HexNAc)4 (Deoxyhexose)3 + (Man)3(GlcNAc)2 (Hex)2 (HexNAc)1 (Deoxyhexose)3 (NeuAc)2 + (Man)3(GlcNAc)2
2861.1	(Hex)2 (HexNAc)6 (Deoxyhexose)1 + (Man)3(GlcNAc)2 (Hex)2 (HexNAc)3 (Deoxyhexose)1 (NeuAc)2 + (Man)3(GlcNAc)2
2877.1	(Hex)3 (HexNAc)3 (NeuAc)2 + (Man)3(GlcNAc)2 (Hex)1 (HexNAc)1 (Deoxyhexose)5 (NeuAc)2 + (Man)3(GlcNAc)2
3182.2	(Hex)3 (HexNAc)3 (NeuAc)3 + (Man)3(GlcNAc)2

[a] ND: not determined.

were observed (Figure 2B,C). However, progression-free survival (PFS) was significantly longer in the high FUCA activity group (>4.3 U/L) than in the low FUCA activity group ($p < 0.05$, Figure 2D). Although plasma FUCA activity was not correlated with the clinical response to trastuzumab, it may be useful as a biomarker for predicting the PFS of for trastuzumab treatment.

Low Expression of Plasma 2534 *m/z* N-Glycan Correlated with Unfavorable Clinical Outcome. We collected plasma N-glycans using glycoblotting-based glycan enrichment[31] and measured their MALDI-TOF-MS peaks. Thirty-one major peaks of N-glycan, observed in over 50% of the patients, were identified (Table 2). Representative data are shown in Figure 3 (left panel). A statistical analysis comparing each peak with the clinical outcome revealed that the expression of plasma 2534 *m/z* N-glycan was significantly lower in patients with progressive disease (PD) ($p < 0.05$, Figure 4A). Low expression of 2534 *m/z* N-glycan discriminated between PD and non-PD with 75% sensitivity and 82% specificity. The expressions of plasma 2534 *m/z* N-glycan in the PD and non-PD groups were 4.3 ± 8.1 and 16.1 ± 11.6 (% of control), respectively. Representative data of 2534 *m/z* N-glycan from six patients are shown in Figure 3 (right panel). In addition, patients with a low expression (not detectable at 2534 *m/z*) of plasma 2534 *m/z* N-glycan exhibited a significantly short PFS ($p < 0.05$, Figure 4B). These results suggest that a low plasma 2534 *m/z* N-glycan level is associated with a poor clinical outcome and that plasma 2534 *m/z* N-glycan may be a predictive biomarker in breast cancer patients treated with trastuzumab.

Discussion

In this study, we investigated predictive biomarkers of response to trastuzumab monotherapy in breast cancer patients, focusing on the processes of fucosylation and glycosylation. Shah et al. reported that serum FUCA activity levels varied in normal, precancerous, and malignant conditions, and suggested that serum FUCA activity might be a useful marker for early detection and for monitoring treatment response in oral cancer patients.[32] We found that a higher plasma FUCA activity level was correlated with a favorable PFS, but that the plasma FUT8 levels was not correlated with clinical response and PFS in breast cancer patients who received trastuzumab treatment. Although the precise mechanisms responsible for our results remain unclear, we speculated that the resulting plasma FUT8 level was not correlated with the clinical outcome because FUT8 catalytic activity occurs strictly in the Golgi apparatus and requires GDP-fucose. On the other hand, the FUCA enzyme has two isoforms, FUCA1 (fucosidase, alpha-L-1, tissue) and FUCA2 (fucosidase, alpha-L-2, plasma). Because FUCA2 is secreted into the plasma,[33] it may influence the phenotype of cancer cells, thereby explaining its correlation with clinical outcome. Indeed, the mRNA expression of FUCA2 was higher and that of FUCA1 was lower in biopsy specimens of gastric cancer, compared with paired noncancerous gastric mucosa (data not shown).

Many researchers have reported new methods for performing glycan structural analyses using mass spectrometry.[34,35] Our method of examining N-glycan profiles utilizes only small amount of plasma sample, making it easy to analyze clinical samples. Several reports have demonstrated that analyzing the glycan structures of proteins in human sera can reveal novel tumor markers in cancer.[11,36] Kyselova et al. reported that several N-glycan structures appear to indicate cancer progression in breast cancer, suggesting that N-glycan profiling of serum may be a useful approach for staging the progression of cancer.[37] An et al. reported that oligosaccharide profiling data using sera samples from patients with ovarian cancer patients and normal controls demonstrated the presence of several unique serum glycan markers in all the patients but not in the normal samples.[38] They mentioned that one major advantage of this approarch is that the glycans can be examined

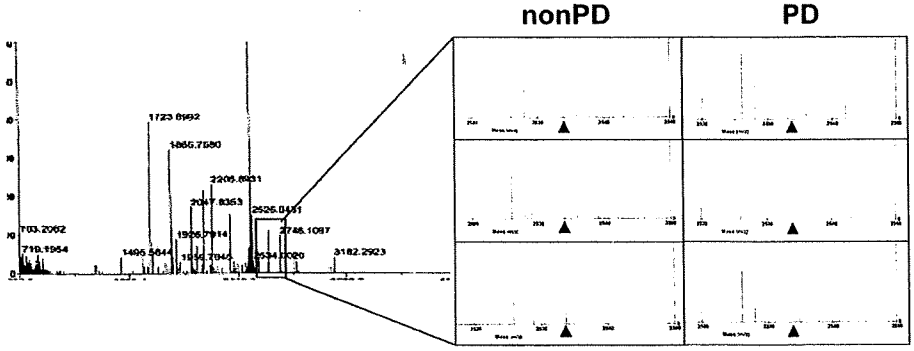

Figure 3. Representative data of plasma N-glycan profile measured using MALDI-TOF-MS (left panel). Twenty-seven microliters of plasma sample was used for the analysis. The mixture was trypsinized and reacted using *N*-glycosidase F. Internal N-glycan standard was added, and the mixture was purified using glycoblotting-based glycan enrichment. The purified samples were measured using MALDI-TOF-MS in reflector, positive ion mode. The number of laser shots was 300 × 2 shots, and the mass range acquired was 700–5000 Da. The N-glycan structure was determined using the GlycoSuite online database, proteome System. All the plasma N-glycans peaks obtained from MALDI-TOF-MS were normalized using the internal standard. The identified 2534 *m/z* N-glycan peaks are shown in six plasma samples (right panel). ▲, 2534 *m/z*; PD, progressive disease.

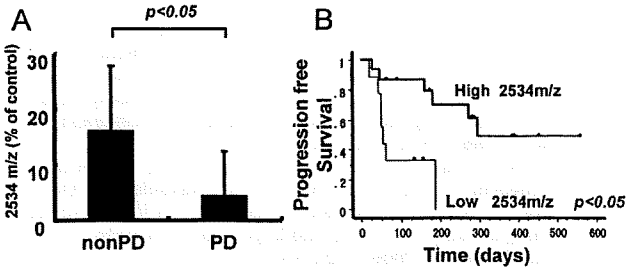

Figure 4. Plasma 2534 *m/z* N-glycan and clinical outcome. (A) Expression of plasma 2534 *m/z* N-glycan and clinical response. The expression of plasma 2534 *m/z* N-glycan was significantly lower ($p < 0.05$) in patients with progressive disease (PD). (B) Kaplan–Meier curve of high (detectable) or low (not detectable) plasma 2534 *m/z* N-glycan groups for progression-free survival (PFS) after trastuzumab treatment. The patients with a low expression of plasma 2534 *m/z* N-glycan exhibited a significantly shorter PFS ($p < 0.05$).

using a serum samples, and cancer biopsy specimens are not needed. In the present study, when the plasma N-glycan profiles of breast cancer patients were examined using MALDI-TOF-MS, 2534 *m/z* N-glycan was found to be correlated with clinical response and PFS. The estimated structure of the identified 2534 *m/z* N-glycan is (Hex)5(HexNAc)2(Deoxyhexose)1 + (Man)3(GlcNAc)2 according to a database (http://au.expasy.org/tools/glycomod/). The experimental confirmation of the predicted structure of 2534 *m/z* is very important. Although we no longer have enough plasma samples to determine the experimental confirmation of structure, we plan to examine 2534 N-glycan in clinical samples to give the experimental confirmation in the future prospective study. This N-glycan has also been found in plasma samples from patients with pancreas cancer, pancreatitis and obstructive bile duct disease (data not shown). We are now investigating the biological mechanism of this N-glycan modification.

In conclusion, we demonstrated that plasma FUCA activity and plasma N-glycan are correlated with the clinical outcome of breast cancer patients treated with trastuzumab. N-Glycan profiles raise the possibility of identifying novel predictive biomarkers for antibody therapy, although a validation study with a larger sample size is needed. Our results show the utility of glycosylation analysis for clinical cancer therapy and provide a novel insight into biomarker studies using glycobiological tools in the field of breast cancer.

Acknowledgment. The following people have played very important roles in the outcome of this project: Hisao Fukumoto, Tatsu Shimoyama, Naoki Hayama, Hideharu Kimura, Masayuki Takeda, Junya Fukai, Kazuko Sakai and Terufumi Kato. We also thank Dr. Richard Simon and Dr. Amy Peng for providing the BRB ArrayTools software. We thank Mr. Hideyuki Shimaoka and Mr. Kazuhiko Fujiwara (Sumitomo Bakelite Co., Ltd.) for their technical support and useful advice. We also thank Mrs. Eiko Honda (Life Science Research Institute, Kinki University) for assistance with the experiments. This work was supported by funds for Health and Labor Scientific Research Grants, Research on Advanced Medical Technology H17-Pharmaco-006 and for the Third-Term Comprehensive 10-Year Strategy for Cancer Control. K.M. is the recipient of a Research Resident Fellowship from the Foundation of Promotion of Cancer Research in Japan.

References

(1) Hakomori, S. Glycosylation defining cancer malignancy: new wine in an old bottle. *Proc. Natl. Acad. Sci. U.S.A.* **2002**, *99* (16), 10231–3.
(2) Ono, M.; Hakomori, S. Glycosylation defining cancer cell motility and invasiveness. *Glycoconjugate J.* **2004**, *20* (1), 71–8.
(3) Zhao, Y. Y.; Takahashi, M.; Gu, J. G.; Miyoshi, E.; Matsumoto, A.; Kitazume, S.; Taniguchi, N. Functional roles of N-glycans in cell signaling and cell adhesion in cancer. *Cancer Sci.* **2008**, *99* (7), 1304–10.
(4) Hakomori, S. Tumor malignancy defined by aberrant glycosylation and sphingo(glyco)lipid metabolism. *Cancer Res.* **1996**, *56* (23), 5309–18.
(5) Contessa, J. N.; Bhojani, M. S.; Freeze, H. H.; Rehemtulla, A.; Lawrence, T. S. Inhibition of N-linked glycosylation disrupts receptor tyrosine kinase signaling in tumor cells. *Cancer Res.* **2008**, *68* (10), 3803–9.
(6) Guo, H. B.; Randolph, M.; Pierce, M. Inhibition of a specific N-glycosylation activity results in attenuation of breast carcinoma cell invasiveness-related phenotypes: inhibition of epidermal growth factor-induced dephosphorylation of focal adhesion kinase. *J. Biol. Chem.* **2007**, *282* (30), 22150–62.
(7) Qiu, Y.; Patwa, T. H.; Xu, L.; Shedden, K.; Misek, D. E.; Tuck, M.; Jin, G.; Ruffin, M. T.; Turgeon, D. K.; Synal, S.; Bresalier, R.; Marcon, N.; Brenner, D. E.; Lubman, D. M. Plasma glycoprotein profiling for colorectal cancer biomarker identification by lectin glycoarray and lectin blot. *J. Proteome Res.* **2008**, *7* (4), 1693–703.

(8) Abbott, K. L.; Aoki, K.; Lim, J. M.; Porterfield, M.; Johnson, R.; O'Regan, R. M.; Wells, L.; Tiemeyer, M.; Pierce, M. Targeted glycoproteomic identification of biomarkers for human breast carcinoma. *J. Proteome Res.* **2008**, *7* (4), 1470–80.
(9) Heo, S. H.; Lee, S. J.; Ryoo, H. M.; Park, J. Y.; Cho, J. Y. Identification of putative serum glycoprotein biomarkers for human lung adenocarcinoma by multilectin affinity chromatography and LC-MS/MS. *Proteomics* **2007**, *7* (23), 4292–302.
(10) Nakagawa, T.; Uozumi, N.; Nakano, M.; Mizuno-Horikawa, Y.; Okuyama, N.; Taguchi, T.; Gu, J.; Kondo, A.; Taniguchi, N.; Miyoshi, E. Fucosylation of N-glycans regulates the secretion of hepatic glycoproteins into bile ducts. *J. Biol. Chem.* **2006**, *281* (40), 29797–806.
(11) Ueda, K.; Katagiri, T.; Shimada, T.; Irie, S.; Sato, T. A.; Nakamura, Y.; Daigo, Y. Comparative profiling of serum glycoproteome by sequential purification of glycoproteins and 2-nitrobenzensulfenyl (NBS) stable isotope labeling: a new approach for the novel biomarker discovery for cancer. *J. Proteome Res.* **2007**, *6* (9), 3475–83.
(12) Li, D.; Mallory, T.; Satomura, S. AFP-L3: a new generation of tumor marker for hepatocellular carcinoma. *Clin. Chim. Acta* **2001**, *313* (1–2), 15–9.
(13) Yamaguchi, Y.; Fujii, J.; Inoue, S.; Uozumi, N.; Yanagidani, S.; Ikeda, Y.; Egashira, M.; Miyoshi, O.; Niikawa, N.; Taniguchi, N. Mapping of the alpha-1,6-fucosyltransferase gene, FUT8, to human chromosome 14q24.3. *Cytogenet. Cell Genet.* **1999**, *84* (1–2), 58–60.
(14) Yamane-Ohnuki, N.; Kinoshita, S.; Inoue-Urakubo, M.; Kusunoki, M.; Iida, S.; Nakano, R.; Wakitani, M.; Niwa, R.; Sakurada, M.; Uchida, K.; Shitara, K.; Satoh, M. Establishment of FUT8 knockout Chinese hamster ovary cells: an ideal host cell line for producing completely defucosylated antibodies with enhanced antibody-dependent cellular cytotoxicity. *Biotechnol. Bioeng.* **2004**, *87* (5), 614–22.
(15) Niwa, R.; Hatanaka, S.; Shoji-Hosaka, E.; Sakurada, M.; Kobayashi, Y.; Uehara, A.; Yokoi, H.; Nakamura, K.; Shitara, K. Enhancement of the antibody-dependent cellular cytotoxicity of low-fucose IgG1 Is independent of FcgammaRIIIa functional polymorphism. *Clin. Cancer Res.* **2004**, *10* (18 Pt 1), 6248–55.
(16) Suzuki, E.; Niwa, R.; Saji, S.; Muta, M.; Hirose, M.; Iida, S.; Shiotsu, Y.; Satoh, M.; Shitara, K.; Kondo, M.; Toi, M. A nonfucosylated anti-HER2 antibody augments antibody-dependent cellular cytotoxicity in breast cancer patients. *Clin. Cancer Res.* **2007**, *13* (6), 1875–82.
(17) Giardina, M. G.; Matarazzo, M.; Morante, R.; Lucariello, A.; Varriale, A.; Guardasole, V.; De Marco, G. Serum alpha-L-fucosidase activity and early detection of hepatocellular carcinoma: a prospective study of patients with cirrhosis. *Cancer.* **1998**, *83* (12), 2468–74.
(18) Ayude, D.; Paez De La Cadena, M.; Martinez-Zorzano, V. S.; Fernandez-Briera, A.; Rodriguez-Berrocal, F. J. Preoperative serum alpha-L-fucosidase activity as a prognostic marker in colorectal cancer. *Oncology* **2003**, *64* (1), 36–45.
(19) Ayude, D.; Fernandez-Rodriguez, J.; Rodriguez-Berrocal, F. J.; Martinez-Zorzano, V. S.; de Carlos, A.; Gil, E.; Paez de La Cadena, M. Value of the serum alpha-L-fucosidase activity in the diagnosis of colorectal cancer. *Oncology* **2000**, *59* (4), 310–6.
(20) Slamon, D. J.; Clark, G. M.; Wong, S. G.; Levin, W. J.; Ullrich, A.; McGuire, W. L. Human breast cancer: correlation of relapse and survival with amplification of the HER-2/neu oncogene. *Science* **1987**, *235* (4785), 177–82.
(21) Seshadri, R.; Firgaira, F. A.; Horsfall, D. J.; McCaul, K.; Setlur, V.; Kitchen, P. Clinical significance of HER-2/neu oncogene amplification in primary breast cancer. The South Australian Breast Cancer Study Group. *J Clin Oncol.* **1993**, *11* (10), 1936–42.
(22) Menard, S.; Pupa, S. M.; Campiglio, M.; Tagliabue, E. Biologic and therapeutic role of HER2 in cancer. *Oncogene* **2003**, *22* (42), 6570–8.
(23) Vogel, C. L.; Cobleigh, M. A.; Tripathy, D.; Gutheil, J. C.; Harris, L. N.; Fehrenbacher, L.; Slamon, D. J.; Murphy, M.; Novotny, W. F.; Burchmore, M.; Shak, S.; Stewart, S. J.; Press, M. Efficacy and safety of trastuzumab as a single agent in first-line treatment of HER2-overexpressing metastatic breast cancer. *J. Clin. Oncol.* **2002**, *20* (3), 719–26.
(24) Hurley, J.; Doliny, P.; Reis, I.; Silva, O.; Gomez-Fernandez, C.; Velez, P.; Pauletti, G.; Powell, J. E.; Pegram, M. D.; Slamon, D. J. Docetaxel, cisplatin, and trastuzumab as primary systemic therapy for human epidermal growth factor receptor 2-positive locally advanced breast cancer. *J. Clin. Oncol.* **2006**, *24* (12), 1831–8.
(25) Naruse, I.; Fukumoto, H.; Saijo, N.; Nishio, K. Enhanced anti-tumor effect of trastuzumab in combination with cisplatin. *Jpn. J. Cancer Res.* **2002**, *93* (5), 574–81.
(26) Kimura, H.; Sakai, K.; Arao, T.; Shimoyama, T.; Tamura, T.; Nishio, K. Antibody-dependent cellular cytotoxicity of cetuximab against tumor cells with wild-type or mutant epidermal growth factor receptor. *Cancer Sci.* **2007**, *98* (8), 1275–80.
(27) Kimura, H.; Kasahara, K.; Kawaishi, M.; Kunitoh, H.; Tamura, T.; Holloway, B.; Nishio, K. Detection of epidermal growth factor receptor mutations in serum as a predictor of the response to gefitinib in patients with non-small-cell lung cancer. *Clin. Cancer Res.* **2006**, *12* (13), 3915–21.
(28) Arao, T.; Fukumoto, H.; Takeda, M.; Tamura, T.; Saijo, N.; Nishio, K. Small in-frame deletion in the epidermal growth factor receptor as a target for ZD6474. *Cancer Res.* **2004**, *64* (24), 9101–4.
(29) Matsumoto, K.; Yokote, H.; Arao, T.; Maegawa, M.; Tanaka, K.; Fujita, Y.; Shimizu, C.; Hanafusa, T.; Fujiwara, Y.; Nishio, K. N-Glycan fucosylation of epidermal growth factor receptor modulates receptor activity and sensitivity to epidermal growth factor receptor tyrosine kinase inhibitor. *Cancer Sci.* **2008**, *99* (8), 1611–17.
(30) Uozumi, N.; Teshima, T.; Yamamoto, T.; Nishikawa, A.; Gao, Y. E.; Miyoshi, E.; Gao, C. X.; Noda, K.; Islam, K. N.; Ihara, Y.; Fujii, S.; Shiba, T.; Taniguchi, N. A fluorescent assay method for GDP-L-Fuc:N-acetyl-beta-D-glucosaminide alpha 1−6fucosyltransferase activity, involving high performance liquid chromatography. *J. Biochem.* **1996**, *120* (2), 385–92.
(31) Miura, Y.; Hato, M.; Shinohara, Y.; Kuramoto, H.; Furukawa, J.; Kurogochi, M.; Shimaoka, H.; Tada, M.; Nakanishi, K.; Ozaki, M.; Todo, S.; Nishimura, S. BlotGlycoABCTM, an integrated glycoblotting technique for rapid and large scale clinical glycomics. *Mol. Cell. Proteomics* **2008**, *7* (2), 370–7.
(32) Shah, M.; Telang, S.; Raval, G.; Shah, P.; Patel, P. S. Serum fucosylation changes in oral cancer and oral precancerous conditions: alpha-L-fucosidase as a marker. *Cancer* **2008**, *113* (2), 336–46.
(33) Ng, W. G.; Donnell, G. N.; Koch, R.; Bergren, W. R. Biochemical and genetic studies of plasma and leukocyte alpha-L-fucosidase. *Am. J. Hum. Genet.* **1976**, *28* (01), 42–50.
(34) Zhao, J.; Qiu, W.; Simeone, D. M.; Lubman, D. M. N-linked glycosylation profiling of pancreatic cancer serum using capillary liquid phase separation coupled with mass spectrometric analysis. *J. Proteome Res.* **2007**, *6* (3), 1126–38.
(35) Zhao, J.; Simeone, D. M.; Heidt, D.; Anderson, M. A.; Lubman, D. M. Comparative serum glycoproteomics using lectin selected sialic acid glycoproteins with mass spectrometric analysis: application to pancreatic cancer serum. *J. Proteome Res.* **2006**, *5* (7), 1792–802.
(36) Isailovic, D.; Kurulugama, R. T.; Plasencia, M. D.; Stokes, S. T.; Kyselova, Z.; Goldman, R.; Mechref, Y.; Novotny, M. V.; Clemmer, D. E. Profiling of human serum glycans associated with liver cancer and cirrhosis by IMS-MS. *J. Proteome Res.* **2008**, *7* (3), 1109–17.
(37) Kyselova, Z.; Mechref, Y.; Kang, P.; Goetz, J. A.; Dobrolecki, L. E.; Sledge, G. W.; Schnaper, L.; Hickey, R. J.; Malkas, L. H.; Novotny, M. V. Breast cancer diagnosis and prognosis through quantitative measurements of serum glycan profiles. *Clin Chem.* **2008**, *54* (7), 1166–75.
(38) An, H. J.; Miyamoto, S.; Lancaster, K. S.; Kirmiz, C.; Li, B.; Lam, K. S.; Leiserowitz, G. S.; Lebrilla, C. B. Profiling of glycans in serum for the discovery of potential biomarkers for ovarian cancer. *J. Proteome Res.* **2006**, *5* (7), 1626–35.

PR800655P

Epidermal growth factor receptor lacking C-terminal autophosphorylation sites retains signal transduction and high sensitivity to epidermal growth factor receptor tyrosine kinase inhibitor

Mari Maegawa,[1,2] Tokuzo Arao,[1] Hideyuki Yokote,[1] Kazuko Matsumoto,[1] Kanae Kudo,[1] Kaoru Tanaka,[1] Hiroyasu Kaneda,[1] Yoshihiko Fujita,[1] Fumiaki Ito[2] and Kazuto Nishio[1,3]

[1]Department of Genome Biology, Kinki University School of Medicine, 377-2 Ohno-Higashi, Osaka Sayama, Osaka, 589-8511; [2]Department of Biochemistry, Setsunan University, 45-1 Nagaotoge-cho Hirakata, Osaka, 573-0101 Japan

(Received September 30, 2008/Revised November 19, 2008/Accepted November 29, 2008)

Constitutively active mutations of epidermal growth factor receptor (EGFR) (delE746_A750) activate downstream signals, such as ERK and Akt, through the phosphorylation of tyrosine residues in the C-terminal region of EGFR. These pathways are thought to be important for cellular sensitivity to EGFR tyrosine kinase inhibitors (TKI). To examine the correlation between phosphorylation of the tyrosine residues in the C-terminal region of EGFR and cellular sensitivity to EGFR TKI, we used wild-type (wt) EGFR, as well as the following constructs: delE746_A750 EGFR; delE746_A750 EGFR with substitution of seven tyrosine residues to phenylalanine in the C-terminal region; and delE746_A750 EGFR with a C-terminal truncation at amino acid 980. These constructs were transfected stably into HEK293 cells and designated HEK293/Wt, HEK293/D, HEK293/D7F, and HEK293/D-Tr, respectively. The HEK293/D cells were found to be 100-fold more sensitive to EGFR TKI (AG1478) than HEK293/Wt. Surprisingly, the HEK293/D7F and HEK293/D-Tr cells, transfected with EGFR lacking the C-terminal autophosphorylation sites, retained high sensitivity to EGFR TKI. In these three high-sensitivity cells, the ERK pathway was activated without ligand stimulation, which was inhibited by EGFR TKI. In addition, although EGFR in the HEK293/D7F and HEK293/D-Tr cells lacked significant tyrosine residues for EGFR signal transduction, phosphorylation of Src homology and collagen homology (Shc) was spontaneously activated in these cells. Our results indicate that tyrosine residues in the C-terminal region of EGFR are not required for cellular sensitivity to EGFR TKI, and that an as-yet-unknown signaling pathway of EGFR may exist that is independent of the C-terminal region of EGFR. (*Cancer Sci* 2009)

Epidermal growth factor receptor (EGFR), also termed HER1/ErbB-1, is overexpressed and activated in many cancers.[1–3] Small-molecule inhibitors of EGFR tyrosine kinase and antibodies have been shown to exhibit antitumor activity in several tumors.[4–6] Somatic mutations of EGFR tyrosine kinase in non-small cell lung cancer have been shown to be associated with hyperresponsiveness to gefitinib, a selective EGFR tyrosine kinase inhibitor (TKI).[7,8] Many investigators have subsequently reported that EGFR mutations are strong determinants of the tumor response to EGFR TKI.[9,10] Approximately 90% of non-small cell lung cancer-associated EGFR mutations in two reports consisted of two major EGFR mutations, namely, delE746_A750 in exon 19 and L858R in exon 21.[11] We previously reported hypersensitivity to EGFR TKI of a PC-9 cell line with delE746_A750 in exon 19, one of the commonly encountered mutations mentioned above, and this deletion mutant of EGFR was constitutively active and activated the ERK and Akt pathway.[12–16] Binding of the receptor with its ligand leads to homodimerization and heterodimerization of the receptor tyrosine kinase.[17,18] Thus, EGFR is a ligand-activated tyrosine kinase that ultimately delivers cellular growth signals.

Tyr-1068, Tyr-1148, and Tyr-1173 in the C-terminal region are the major autophosphorylation sites in human EGFR. These C-terminal phosphorylation sites of EGFR interact with adaptor proteins.[19,20] Phosphorylation of the C-terminal autophosphorylation sites of EGFR, triggered by epidermal growth factor (EGF), in turn trigger an intracellular signal cascade involving proteins such as ERK, Akt, Janus kinase, and signal transducer and activator of transcription.[15,21,22] Src homology and collagen homology (Shc) is a molecular adaptor protein that binds phosphorylated tyrosines within activated EGFR, and is itself phosphorylated on tyrosine residues upon stimulation of EGFR. The phosphorylated CH1 site of Shc then engages the binding site for the SH2 domain of growth factor receptor-bound protein (Grb) 2. The SH3 domain of Grb2 directly interacts with the guanyl nucleotide exchange factor son of sevenless homolog (Sos).[23,24] Sos catalyzes the conversion of GDP to GTP on Ras, resulting in Ras activation. Activated GTP-Ras recruits Raf kinase to the plasma membrane, resulting in Raf activation and phosphorylation of its downstream target ERK kinase.[25,26]

Phosphorylation of tyrosine residues at the C-terminal region of EGFR is believed to be important in cell signaling triggered by wild-type EGFR.[27,28] However, the role of this region in an active mutant of EGFR (delE746_A750) has yet to be elucidated in detail. To clarify the biological functions of the tyrosine residues at the C-terminal region of EGFR, we constructed several mutants with C-terminal-truncated or substitution of tyrosine residues to phenylalanine in the C-terminal region. We showed that EGFR lacking C-terminal autophosphorylation sites still generated signals, with retention of cellular hypersensitivity to EGFR TKI.

Materials and Methods

Expression constructs. The method used to obtain full-length cDNA of wild-type *EGFR* has been described previously.[12] Wild-type *EGFR* cDNA and 15 bp-deletion *EGFR* (delE746_A750) were introduced into pcDNA3.1 (Invitrogen, Carlsbad, CA, USA) with a myc-tag at its C-terminus. The *EGFR* cDNA with substitution of seven tyrosine residues to phenylalanine in the C-terminal region was amplified by mutagenesis; the QuikChange®

[3]To whom correspondence should be addressed. E-mail: knishio med.kindai.ac.jp

doi: 10.1111/j.1349-7006.2008.01071.x

Site-Directed Mutagenesis Kit (Stratagene, La Jolla, CA, USA) was used for the polymerase chain reaction and a primer set was synthesized (Supporting Information Table S1). The cDNA of the C-terminal-truncated *EGFR* with 15-bp deletion (*EGFR-D-Tr*) was amplified using the following primer set: forward, CCT CCT CTT GCT GCT GGT GGT G; reverse, GAA CAAGCT TGA CAA GGT AGC GCT GGG GGT CTC. After the polymerase chain reaction products were cut with *Cla*I and *Hind*III, they were ligated to the *Cla*I and *Hind*III sites of the pcDNA3.1 expression vector containing EGFR-D cDNA. The cDNA of wild-type *EGFR* with the C-terminal truncation at amino acid 980 (*EGFR-Wt-Tr*) was made from the *Cla*I and *Xho*I fragments of the pcDNA3.1 expression vector containing wild-type EGFR and the *Cla*I and *Xho*I fragments of the pcDNA3.1 expression vector containing *EGFR-D-Tr*.

Epidermal growth factor receptor cDNA with the myc-tag in pcDNA3.1 was cut and introduced into a pQCLIN retroviral vector (BD Biosciences Clontech, San Diego, CA, USA) together with enhanced green fluorescent protein (EGFP) followed by the internal ribosome entry sequence, to monitor the expression of the inserts indirectly. A pVSV-G vector (Clontech, Palo Alto, CA, USA) for constitution of the viral envelope, pGP vector (Takara, Yotsukaichi, Japan), and the pQCXIX constructs were cotransfected into HEK293 cells using FuGENE6 transfection reagent (Roche Diagnostics, Basel, Switzerland). Briefly, 80% confluent cells cultured in a 10-cm dish were transfected with 2 μg pVSV-G vector plus 6 μg pQCXIX vector. Forty-eight hours after the transfection, the culture medium was collected and the viral particles were concentrated by centrifugation at 15 000*g* for 3 h at 4°C. The viral pellet was then resuspended in fresh Dulbecco's modified Eagle's medium (DMEM; Sigma, St Louis, MO, USA). The titer of the viral vector was calculated by counting the EGFP-positive cells that were infected in serial dilutions of a virus-containing medium and then determining the multiplicity of infection. HER2 and HER3 introduced retrovirally into HEK293 cells were used as positive controls in western blotting.

Cell culture and transfection. The human embryonic kidney HEK293 cell line was obtained from the American Type Culture Collection (Manassas, VA, USA) and cultured in DMEM supplemented with 10% fetal bovine serum, penicillin, and streptomycin (Sigma) in a humidified atmosphere of 5% CO_2 at 37°C. The HEK293 cells were transfected with the viral vectors.

***In vitro* growth-inhibition assay.** The growth-inhibitory effects of AG1478 (Biomol International, Plymouth Meeting, PA, USA) in HEK293/Wt, HEK293/Wt-Tr, HEK293/D, HEK293/D7F, and HEK293/D-Tr cells were examined using a 3, 4, 5-dimethyl-2H-tetrazolium bromide (MTT) assay as described previously.[29]

Immunoprecipitation. The culture cells were washed twice with ice-cold phosphate-buffered saline (PBS) (–), and lysed with a lysis buffer containing 20 mM Tris-HCl (pH 7.0), 50 mM NaCl, 5 mM ethylenediaminetetraacetic acid, 10 mM Na pyrophosphate, 50 mM NaF, 1 mM Na orthovanadate, 1% TritonX-100, and the Complete Mini protease inhibitor mix (Roche Diagnostics). The lysates were cleared by centrifugation at 15 000 *g* for 10 min and the protein concentrations of the supernatants were measured using a bicinchoninic acid protein assay (Pierce Biotechnology, Rockford, IL, USA).

The cell lysates (500 μg) were immunoprecipitated by overnight incubation with 3 μg anti-EGFR antibody, anti-HER3 antibody (Upstate Biotechnology, Lake Placid, NY, USA), anti-HER2 antibody (Santa Cruz Biotechnology, Santa Cruz, CA), or anti-c-Myc (Roche Diagnostics), followed by further incubation with protein-G agarose (Santa Cruz Biotechnology) for 1 h. Bound proteins were washed three times with lysis buffer and eluted in Laemmli sample buffer containing 2-mercaptoethanol. The eluted proteins were subjected to 2–15% gradient sodium dodecylsulfate–polyacrylamide gel electrophoresis (SDS-PAGE) and immmunoblotted as described above.

Immunoblotting. Whole-cell lysates and the immunoprecipitates were separated using 2–15% gradient SDS-PAGE and blotted on to a polyvinylidene fluoride membrane. The membrane was probed with anti-EGFR, anti-HER3 (Upstate Biotechnology), anti-phospho(Tyr845)-EGFR, anti-phospho(Tyr1068)-EGFR, anti-phospho(Tyr1173)-EGFR, anti-HER2, anti-phospho-tyrosine, anti-p44/42 mitogen-activated protein (MAP) kinase, anti-phospho-p44/42 MAP kinase, anti-Shc, anti-phospho-Shc (Cell Signaling, Beverly, MA), anti-Sos (Santa Cruz), anti-Grb2 (BD Biosciences, San Jose, CA), and anti-c-Myc (Roche Diagnostics) antibodies by incubation for 2 h at room temperature and then with horseradish peroxidase-conjugated anti-rabbit IgG antibody or anti-mouse IgG antibody for 1 h at room temperature. Finally, the proteins were visualized with an enhanced chemiluminescence western blotting detection system (GE Healthcare, Piscataway, NJ, USA).

Chemical crosslinking assay. After treatment or no treatment with EGF (R&D Systems, Minneapolis, MN, USA) the chemical crosslinking assay was carried out in intact cells as described previously.[13] The transfected cells were washed with ice-cold PBS (+) and incubated for 30 min at room temperature in PBS (+) containing 2 mM crosslinker bis(sulfosuccinimidyl)suberate (Pierce Biotechnology). The reaction was terminated with 20 mM Tris (pH 7.5) for 15 min at room temperature. The cells were washed with PBS (+), and 15 μg protein was resolved by 2–15% gradient SDS-PAGE and then immunoblotted with anti-EGFR and anti-phospho-EGFR antibodies.

Results

Epidermal growth factor receptor lacking C-terminal autophosphorylation sites (EGFR-D-Tr and EGFR-D7F) retains signal transduction. To examine the role of the tyrosine residues in the C-terminal region of EGFR in signal transduction, we constructed vectors containing wild-type EGFR, a deletion mutant (delE746_A750 EGFR) with C-terminal truncation, or a mutant with substitution of seven tyrosine residues in the C-terminal region (Fig. 1a), and transfected these vectors into HEK293 cells with rather low expression levels of endogenous EGFR. The expression of exogenous EGFR in the transfectants was confirmed by immunoblotting with anti-EGFR antibodies (Fig. 1b).

In order to examine the signal transduction of EGFR in the transfectants, we analyzed the phosphorylation status of EGFR and its downstream molecules. Phosphorylation of EGFR at the Y845 and Y1173 tyrosine residues was detected in HEK293/Wt and HEK293/D cells cultivated in medium containing 10% fetal bovine serum (Fig. 2a). Enhanced phosphorylation of the Y1068 tyrosine residue was observed specifically in the HEK293/D cells, suggesting that Y1068 is constitutively active in delE746_A750 EGFR. This phenomenon is consistent with our previous reports.[29,30] On the other hand, no significant phosphorylation of Y845, Y1068, or Y1173 was observed in the HEK293/D7F and HEK293/D-Tr cells. ERK and Akt are major downstream pathways of EGFR. We examined the phosphorylation of ERK and Akt in the transfectants. Increased phosphorylation of ERK was observed in the HEK293/D7F, HEK293/D-Tr, and HEK293/D cells, even though HEK293/D7F and HEK293/D-Tr cells were transfected with EGFR lacking the C-terminal autophosphorylation sites.

We also examined ligand-dependent signals in these cells under the 1% serum starve medium (Fig. 2b). Ligand-stimulated phosphorylation of EGFR was observed in the HEK293/Wt cells transfected with wild-type EGFR. Constitutive phosphorylation of EGFR and a further increase in the EGFR phosphorylation response to EGF were observed in the HEK293/D cells. On the other hand, no significant phosphorylation in response to EGF binding was observed in the HEK293/D7F and HEK293/D-Tr cells. Downstream of EGFR, increased phosphorylation of ERK and Akt was observed in response to EGF in the HEK293/D7F

doi: 10.1111/j.1349-7006.2008.01071.x

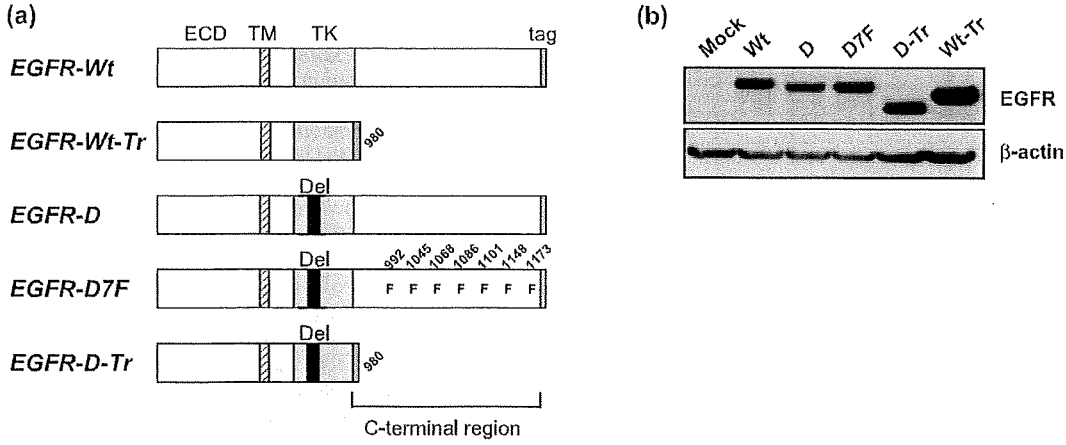

Fig. 1. Epidermal growth factor receptor (EGFR) constructs and their expression. (a) Structures of the various EGFR mutants. EGFR-Wt, wild-type human EGFR; EGFR-Wt-Tr, wild-type kinase domain of EGFR with C-terminal truncation at amino acid 980; EGFR-D, EGFR with a 15-bp deletion from the tyrosine kinase domain (delE746_A750); EGFR-D7F, 15-bp deletion of EGFR (delE746_A750) and substitution of seven tyrosine residues to phenylalanine (Y992F, Y1068F, Y1045F, Y1068F, Y1086F, Y1148F, Y1173F); and EGFR-D-Tr, 15-bp deletion of EGFR (delE746_A750) with C-terminal truncation at amino acid 980. EGFR-Wt, EGFR-D, EGFR-D7F, and EGFR-D-Tr contained a myc-tag. EGFR-Wt-Tr contained a flag-tag. ECD, extracellular domain; TK, tyrosine kinase; TM, transmembrane. (b) Stable transfectants were lysed and cell lysates containing equal amounts of protein were immunoblotted with anti-EGFR antibody recognizing the extracellular domain of EGFR. A band with a molecular weight of ~170 kDa was detected in the HEK293/Wt, HEK293/D, and HEK293/D7F cells, and a band of lower molecular weight was detected in the HEK293/D-Tr and HEK293/Wt-Tr cells. Mock, HEK293/Mock; Wt, HEK293/Wt; Wt-Tr, HEK293/Wt-Tr; D, HEK293/D; D7F, HEK293/D7F; and D-Tr, HEK293/D-Tr.

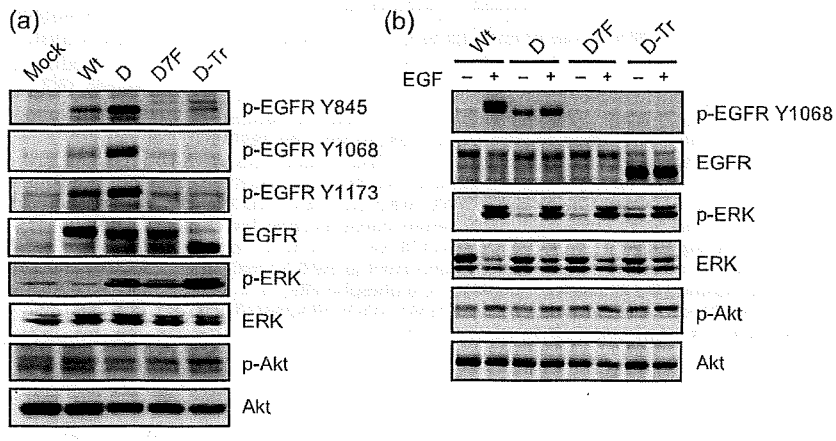

Fig. 2. Epidermal growth factor receptor (EGFR) lacking C-terminal autophosphorylation sites retains EGFR signal transduction. (a) The HEK293/Mock, HEK293/Wt, HEK293/D, HEK293/D7F, and HEK293/D-Tr cells were lysed, and the cell lysates were immunoblotted with anti-phospho-EGFR (p-EGFR Y845, Y1068, Y1173), anti-EGFR (recognizing the extracellular domain), anti-phospho-ERK, anti-ERK, anti-phospho-Akt, and anti-Akt antibodies. (b) The HEK293/Wt, HEK293/D, HEK293/D7F, and HEK293/D-Tr cells were incubated in 1% serum starve medium for 12 h, followed by treatment with 10 ng/mL epidermal growth factor for 10 min at 37°C. The cell lysates were immunoblotted. Mock, HEK293/Mock; Wt, HEK293/Wt; D, HEK293/D; D7F, HEK293/D7F; and D-Tr, HEK293/D-Tr.

and HEK293/D-Tr cells, as well as the HEK293/Wt and HEK293/D cells. These results indicate that EGFR lacking the C-terminal autophosphorylation sites (EGFR-D-Tr and EGFR-D7F) retained signal transduction ability.

Transfectants with EGFR lacking C-terminal autophosphorylation sites retain their hypersensitivity to EGFR TKI. EGF stimulation increased the growth of HEK293/Wt cells significantly but did not affect their sensitivity to AG1478 (data not shown). To examine the role of the C-terminal region of EGFR in cellular sensitivity to EGFR TKI, the sensitivity of these transfectants was examined by growth-inhibition assay (Fig. 3a). HEK293/Wt and HEK293/Wt-Tr cells with normal EGFR in relation to the kinase domain were relatively resistant to EGFR TKI, with IC_{50} values of 3.0 ± 0.97 and 8.1 ± 0.99 μM. On the other hand, HEK293/D (0.028 ± 0.018 μM), HEK293/D7F (0.047 ± 0.030 μM), and HEK293/D-Tr (0.017 ± 0.017 μM) cells were ~100 times more sensitive to AG1478 compared to HER293/Wt cells (Fig. 3a), suggesting that the cells transfected with EGFR lacking C-terminal phosphorylation sites retained hypersensitivity to EGFR TKI. There were no differences in the proliferation rates of these cell lines under the absence of drug exposure (data not shown).

To elucidate the effect of EGFR TKI on the EGFR-triggered signal cascade, the phosphorylation status of EGFR and ERK was examined in the transfectants treated with AG1478 under the 1% serum starve medium (Fig. 3b). AG1478 at a concentration of 20 nM inhibited the phosphorylation of EGFR in HEK293/D cells, but not in the other cell lines. The increased phosphorylation of ERK observed in the HEK293/D, HEK293/D7F, and HEK293/D-Tr cells was inhibited by AG1478 at 20 nM. These results suggest that signal transduction from C-terminal-truncated EGFR to downstream molecules allows sensitivity to EGFR TKI to be retained, just like the deletion mutant of EGFR (delE746_A750).

Endogenous HER families are not involved in the dimerization of EGFR-D-Tr and EGFR-D7F. We hypothesized that the signals from EGFR lacking the C-terminal autophosphorylation sites were transduced through heterodimerization with endogenous EGFR, HER2, or HER3. No significant endogenous EGFR expression or its phosphorylation was observed in the HEK293/Mock cells (Fig. 4a). Very low levels of intrinsic HER2 or HER3 expression were detected in the HEK293 cells, and the expression levels seemed not to be involved in significant drug sensitivity nor increased signal transduction (Fig. 4b,c). Therefore, it is not likely that heterodimerization of